Breadth of SARS-CoV-2 Neutralization and Protection Induced by a Nanoparticle Vaccine (75 characters)

Dapeng Li[1,2], David R. Martinez[3], Alexandra Schäfer[3], Haiyan Chen[1], Maggie Barr[1], Laura L. Sutherland[1], Esther Lee[1], Robert Parks[1], Dieter Mielke[4], Whitney Edwards[1], Amanda Newman[1,2], Kevin W. Bock[5], Mahnaz Minai[5], Bianca M. Nagata[5], Matthew Gagne[6], Daniel C. Douek[6], C. Todd DeMarco[1,2], Thomas N. Denny[1,2], Thomas H. Oguin III[1,2], Wes Rountree[1,2], Yunfei Wang[1,2], Katayoun Mansouri[1], Robert J. Edwards[1,2], Guido Ferrari[4], Gregory D. Sempowski[1,2], Amanda Eaton[1,4], Juanjie Tang[7], Derek W. Cain[1,2], Sampa Santra[8], Norbert Pardi[9], Drew Weissman[10], Mark A. Tomai[11], Christopher B. Fox[12], Ian N. Moore[5], Hanne Andersen[13], Mark G. Lewis[13], Hana Golding[7], Surender Khurana[7], Robert Seder[6], Ralph S. Baric[3], David C. Montefiori[1,4], Kevin O. Saunders[1,4,14,15,#], Barton F. Haynes[1,2,14,#]

[1]Duke Human Vaccine Institute, Duke University School of Medicine, Durham, NC 27710, USA.

[2]Department of Medicine, Duke University School of Medicine, Durham, NC 27710, USA.

[3]Department of Epidemiology, University of North Carolina at Chapel Hill, Chapel Hill, NC 27599, USA.

[4]Department of Surgery, Duke University School of Medicine, Durham, NC 27710, USA.

[5]Infectious Disease Pathogenesis Section, Comparative Medicine Branch, National Institute of Allergy and Infectious Diseases, National Institutes of Health, Bethesda, MD 20814, USA.

[6]Vaccine Research Center, National Institute of Allergy and Infectious Diseases, National Institutes of Health, Bethesda, MD 20814, USA.

[7]Division of Viral Products, Center for Biologics Evaluation and Research (CBER), Food and Drug Administration, Silver Spring, MD 20871, USA.

[8]Beth Israel Deaconess Medical Center, Boston, MA 02215, USA.

[9]Department of Microbiology, University of Pennsylvania, Philadelphia, PA 19104, USA.

[10]Department of Medicine, University of Pennsylvania, Philadelphia, PA 19104, USA.

[11]Corporate Research Materials Lab, 3M Company, St Paul, MN 55144, USA.

27 [12]Infectious Disease Research Institute, Seattle, WA 98104, USA.

28 [13]BIOQUAL, Rockville, MD 20850, USA.

29 [14]Department of Immunology, Duke University School of Medicine, Durham, NC 27710, USA.

30 [15]Department of Molecular Genetics and Microbiology, Duke University School of Medicine, Durham,

31 NC 27710, USA.

32 [#]Correspondence: kevin.saunders@duke.edu (K.O.S.); barton.haynes@duke.edu (B.F.H.)

33

ABSTRACT (171 words)

Coronavirus vaccines that are highly effective against SARS-CoV-2 variants are needed to control the current pandemic. We previously reported a receptor-binding domain (RBD) sortase A-conjugated ferritin nanoparticle (RBD-scNP) vaccine that induced neutralizing antibodies against SARS-CoV-2 and pre-emergent sarbecoviruses and protected monkeys from SARS-CoV-2 WA-1 infection. Here, we demonstrate SARS-CoV-2 RBD-scNP immunization induces potent neutralizing antibodies in non-human primates (NHPs) against all eight SARS-CoV-2 variants tested including the Beta, Delta, and Omicron variants. The Omicron variant was neutralized by RBD-scNP-induced serum antibodies with a mean of 4.3-fold reduction of ID_{50} titers compared to SARS-CoV-2 D614G. Immunization with RBD-scNPs protected NHPs from SARS-CoV-2 WA-1, Beta, and Delta variant challenge, and protected mice from challenges of SARS-CoV-2 Beta variant and two other heterologous sarbecoviruses. These results demonstrate the ability of RBD-scNPs to induce broad neutralization of SARS-CoV-2 variants and to protect NHPs and mice from multiple different SARS-related viruses. Such a vaccine could provide the needed immunity to slow the spread of and reduce disease caused by SARS-CoV-2 variants such as Delta and Omicron.

KEYWORDS

SARS-CoV-2, Vaccine, Nanoparticle, Neutralizing Antibodies, Protection, Non-human primates

54 **INTRODUCTION**

55 Despite the remarkable success of approved COVID-19 vaccines, additional broadly protective
56 vaccines may be needed to combat breakthrough infections caused by emerging SARS-CoV-2 variants
57 and waning immunity. Moreover, pan-Sarbecovirus vaccines are needed for the prevention of new animal
58 SARS-like viruses that may jump to humans in the future (Levin et al., 2021). Modified mRNA vaccines
59 encapsulated in lipid nanoparticles (LNPs) have proved transformative for COVID-19 vaccine
60 development and for vaccine development in general (Chaudhary et al., 2021; Pardi et al., 2018; Pardi et
61 al., 2020). Developed in 11 months and providing >90% efficacy from transmission, the mRNA-1273 and
62 the BNT162b2 COVID-1 vaccines, while showing the most reduction in efficacy from SARS-CoV-2
63 Beta and Omicron variants, continue to provide significant protection from serious COVID-19 disease,
64 hospitalization, and death (Baden et al., 2021; Haynes, 2021; Polack et al., 2020). The Omicron variant,
65 however, has proved to be more transmissible than previous variants, now accounting for the majority of
66 global isolates (http://www.gisaid.org/hcov19-variants). Likely arising from immunocompromised
67 individuals in South Africa, the Omicron variant spike protein contains 30 mutations compared to the
68 WA-1 strain, and continues to evolve (Wang and Cheng, 2021). While likely less pathogenic than Delta
69 and other SARS-CoV-2 variants, the enhanced transmissibility of Omicron, coupled with the sheer
70 number of resulting cases, has resulted in a higher absolute number of COVID-19 patients compared to
71 previous variant infections, thus providing a continued burden on global health care systems.

72 We previously reported an RBD-based, sortase A-conjugated nanoparticle (RBD-scNP) vaccine
73 formulated with the TLR7/8 agonist 3M-052-aqueous formulation (AF) (hereafter 3M-052-AF) plus
74 Alum, that elicited cross-neutralizing antibody responses against SARS-CoV-2 and other sarbecoviruses,
75 and protected against the WA-1 SARS-CoV-2 strain in non-human primates (NHPs) (Saunders et al.,
76 2021). Here, we found RBD-scNPs induced antibodies that neutralized all variants tested including Beta
77 and Omicron, and protected against Beta and Delta variant challenges in macaques. Moreover, RBD-
78 scNP immunization protected in highly susceptible aged mouse models against challenges of SARS-CoV-
79 2 Beta variant and other betacoronaviruses. In addition, while Alum, 3M-052-AF, or 3M-052-AF + Alum

80 as adjuvant for RBD-scNP each protected animals from WA-1 challenge, the 3M-052-AF/ RBD-scNP
81 formulation was optimal for induction of neutralization titers to variants and protection from lung
82 inflammation. Finally, we found that RBD-, N-terminal domain (NTD)- and spike-2P (S2P)-scNPs each
83 protected comparably in the upper and lower airways from WA-1, but boosting with the NTD-scNP
84 protected less well than RBD- or S2P-scNP.
85
86 **RESULTS**
87 **RBD-scNPs induce neutralizing antibodies against SARS-CoV-2 B.1.1.529 (Omicron) and other**
88 **variants**
89 RBD-scNPs were used to immunize macaques 3 times four weeks apart (***Figure 1A***). To test whether
90 RBD-scNP-induced antibodies can neutralize SARS-CoV-2 variants, we collected macaque plasma
91 samples two weeks after the 3rd RBD-scNP immunization (Saunders *et al.*, 2021) and assessed their
92 ability to neutralize pseudovirus infection of 293T-ACE2-TMPRSS2 cells by SARS-CoV-2 WA-1 and 8
93 variants (***Figure 1A***). RBD-scNP induced potent plasma neutralizing antibodies against the WA-1 strain
94 with geometric mean titer (GMT) ID_{50} of 12,266.7, while reduced ID_{50} titers were observed to different
95 extents for the variants (***Figure 1B-C***). Particularly, the highest reduction of neutralizing activity was
96 observed for the B.1.351 (Beta) variant, which ranged from 4.1- to 10.2- fold (***Figure 1C***). To determine
97 if the B.1.1.529 (Omicron) variant could escape RBD-scNP-induced neutralizing antibodies, we
98 compared immune sera for capacity to neutralize the D614G and Omicron variants in a 293T-ACE2
99 pseudovirus assay. Serum antibodies induced by three doses of RBD-scNP immunization (Saunders *et al.*,
100 2021) neutralized both the D614G (ID_{50}=16,531, ID_{80}=5,484) and Omicron (ID_{50}=3,858, ID_{80}=980)
101 pseudoviruses. A 4.3-fold drop in the ID_{50} GMT and 5.6-fold drop in the ID_{80} GMT were observed
102 (***Figure 1D***). Thus, high titers of neutralizing antibodies against SARS-CoV-2 variants, including
103 Omicron, were elicited by the RBD-scNP immunization in macaques.
104
105 **RBD-scNPs protected macaques from SARS-CoV-2 WA-1, Beta and Delta challenge**

106 Next, we determined if two doses of RBD-scNP vaccination could protect NHPs from challenge by
107 SARS-CoV-2 WA-1, Beta or Delta variants. We immunized cynomolgus macaques with two doses of
108 RBD-scNP vaccine, PBS, or adjuvant alone (***Figure 2A***). We also immunized a group of macaques with
109 soluble RBD as comparators to RBD-scNP immunization to test the effects of multimerization. RBD-
110 scNP and soluble RBD monomer immunization elicited similar titers of antibodies binding to SARS-
111 CoV-2 and other CoV spike antigens (***Supplementary Figure 1A***), which also similarly blocked ACE2-
112 binding on SARS-CoV-2 spike and bat CoV RsSHC014 spike (***Supplementary Figure 1B-C***). RBD-
113 scNPs and soluble RBD induced similar levels of antibodies targeting the sarbecovirus cross-neutralizing
114 DH0147-epitope (Hastie et al., 2021; Li et al., 2021a; Li et al., 2021b; Martinez et al., 2021a) on SARS-
115 CoV-2 spike as well as on RsSHC014 spike (***Supplementary Figure 1B-C***). In pseudovirus neutralization
116 assays, the RBD-scNP group exhibited higher titers of neutralizing antibodies than the soluble RBD
117 group against the WA-1, Alpha, Epsilon, Iota, and Delta viruses, with comparable neutralizing titers
118 against Beta, Gamma, and Kappa variants (***Supplementary Figure 1D***). In both groups, neutralizing titers
119 for the Beta, Gamma, and Iota variants were reduced compared to WA-1 (***Supplementary Figure 1E***).
120 Thus, RBD-scNP induced higher neutralizing antibodies than soluble RBD monomer for 5 out of 8
121 SARS-CoV-2 variant pseudoviruses tested.
122 Two weeks after the second vaccination, macaques (n=5 per group) were challenged with SARS-
123 CoV-2 WA-1, SARS-CoV-2 B.1.351 (Beta) variant, or SARS-CoV-2 B.1.617.2 (Delta) variant (***Figure***
124 ***2A***). In the PBS or adjuvant alone group, high copies of envelope (E) and nucleocapsid (N) gene
125 subgenomic RNA (sgRNA) were detected in both Bronchoalveolar Lavage (BAL) and nasal swab
126 samples collected on day 2 and 4 post-challenge (***Figure 2B-D and Supplementary Figure 1F-H***). In
127 contrast, 5 of 5 animals in the RBD-scNP group, and 4 of 5 animals in the soluble RBD group, were
128 completely protected from WA-1 infection, as indicated by no detectable sgRNA in either BAL or nasal
129 swab (***Figure 2B***). After the SARS-CoV-2 Beta variant challenge, nasal N gene sgRNA was detected in
130 only 1 of 5 of the RBD-scNP immunized monkeys but in 4 of 5 of the soluble RBD immunized monkeys
131 (***Figure 2C***). In addition, after the SARS-CoV-2 Delta variant challenge, all animals that received two

132 doses of RBD-scNP immunization showed no detectable sgRNA in BAL or nasal swab samples (***Figure***
133 ***2D***).

134 Animals were necropsied 4 days after challenge for histopathologic analysis to determine SARS-
135 CoV-2-associated lung inflammation. After WA-1 and Beta variant challenge, lung tissue haematoxylin
136 and eosin (H&E) staining revealed no difference between groups (***Figure 2E-F***). However,
137 immunohistochemistry (IHC) staining showed the presence of SARS-CoV-2 nucleocapsid antigen in the
138 lungs of macaques administered PBS or adjuvant alone, but not in the lungs of RBD-scNP or soluble
139 RBD immunized monkeys (***Figure 2E-F***). Thus, while lung inflammation was observed in immunized
140 macaques, two doses of RBD-scNP immunization protected against viral replication of WA-1, the Beta
141 variant, or Delta variant in both lower and upper airways. In addition, RBD-scNP was superior to soluble
142 RBD in terms of protecting from the hard-to-neutralize Beta variant infection in the upper respiratory
143 tract.

144

145 **RBD-scNPs induce protective responses in mice against SARS-CoV-2 Beta variant and other**
146 **betacoronaviruses**

147 To define the protective efficacy of the RBD-scNP vaccination against different betacoronaviruses,
148 we immunized aged mice with two doses of RBD-scNPs, challenged the mice with mouse-adapted
149 SARS-CoV-2 WA-1, SARS-CoV-2 Beta variant, SARS-CoV-1, or bat CoV RsSHC014 (***Figure 2G***). In
150 the SARS-CoV-2 WA-1 challenge study, RBD-scNP protected mice from weight loss through 4 days post
151 infection (dpi) and protected from viral replication in the lungs (***Figure 2H***). Similar protection from
152 weight loss and lung viral replication were observed in the SARS-CoV-2 Beta variant challenged mice
153 (***Figure 2I***); moreover, by 4 dpi five of the ten unimmunized mice died but no RBD-scNP-immunized
154 mice died. Mice immunized with RBD-scNP were also protected against weight loss induced by SARS-
155 CoV-1 and showed ~3-log lower average PFU titer in lungs compared to adjuvant alone and
156 unimmunized groups (***Figure 2J***). Lastly, RBD-scNP immunization conferred protection against
157 RsSHC014 challenge-induced weight loss and resulted in ~2-log lower average PFU titer than naïve mice

158 (***Figure 2K***). Thus, two doses of RBD-scNP immunization elicited protective immune responses against
159 SARS-CoV-2 Beta variant and multiple other betacoronaviruses in aged mouse models.
160
161 **Adjuvant is required for RBD-scNP induction of potent plasma and mucosal antibody responses**
162 To optimize adjuvant formulations for the RBD-scNP vaccine, we next formulated the RBD-scNP
163 immunogen with the TLR7/8 agonist 3M-052-AF alone, with aluminum hydroxide (Alum) alone, or with
164 3M-052-AF adsorbed to Alum (3M-052-AF + Alum). Control groups included NHPs immunized with
165 immunogen alone (RBD-scNP without adjuvant), adjuvant alone (3M-052-AF, Alum, or 3M-052-AF +
166 Alum without immunogen), or PBS alone (***Figure 3A***). After three immunizations, RBD-scNP alone
167 without adjuvant induced minimal binding antibodies to SARS-CoV-2 and other CoV spike antigens,
168 whereas higher titers of binding antibodies were induced by RBD-scNP formulated with each adjuvant
169 (***Supplementary Figure 2A***). While all three adjuvant formulations were highly immunogenic, RBD-
170 scNP adjuvanted with 3M-052-AF induced the highest DH1047-blocking plasma antibodies ($p < 0.05$;
171 Wilcoxon rank sum exact test; ***Supplementary Figure 2B-C***). Mucosal antibody levels tended to be
172 comparable for macaques who received RBD-scNP formulated with 3M-052-AF or 3M-052+Alum, with
173 only low titers being seen when Alum was used to adjuvant the RBD-scNP (***Supplementary Figure 2D-***
174 ***E***).
175
176 **Robust neutralizing antibodies and *in vivo* protection induced by adjuvanted RBD-scNP**
177 While the RBD-scNP alone group showed minimal neutralizing antibody titers, the RBD-scNP +
178 3M-052-AF group had remarkably high pseudovirus neutralizing antibody titers against SARS-CoV-2
179 WA-1 strain (GMT ID_{50} = 59,497). The GMT ID_{50} of RBD-scNP + 3M-052-Alum and RBD-scNP +
180 Alum groups against WA-1 were 12,267 and 12,610, respectively (***Figure 3B***). Moreover, RBD-scNPs +
181 3M-052-AF immunized animals exhibited the highest magnitudes of neutralizing antibodies against each
182 variant we tested (***Figure 3B***).

183 To compare *in vivo* protection of RBD-scNP with different adjuvant formulations, cynomolgus
184 macaques were challenged with the WA-1 strain of SARS-CoV-2 three weeks after the third
185 immunization (***Figure 3A***). Compared to unimmunized monkeys, the adjuvant alone groups exhibited
186 similar or higher levels of E and N sgRNA, and the RBD-scNP immunogen alone reduced sgRNA copies
187 by only ~1-2 logs (***Figure 3C and Supplementary Figure 2F***). Immunization with either RBD-scNP
188 adjuvanted with 3M-052-AF + Alum or 3M-052-AF conferred robust protection against SARS-CoV-2
189 infection. Macaques in these groups had under-detection-limit or near-baseline levels of sgRNA N and E
190 in both lower and upper respiratory tracts, demonstrating that adjuvant was required for eliciting potent
191 protection from SARS-CoV-2 challenge. RBD-scNP + Alum immunized macaques showed positive E or
192 N gene sgRNA in 1 of 5 and 2 of 5 macaques in BAL samples collected on day 2 post-challenge
193 respectively. By day 4 post-challenge, all RBD-scNP adjuvanted groups showed no detectable sgRNA
194 (***Figure 3C and Supplementary Figure 2F***).
195 Histologic analysis of lung tissue showed that RBD-scNP + adjuvant and adjuvant only groups had
196 similar inflammation scores (***Figure 3D***). IHC staining of the lung tissues exhibited high SARS-CoV-2
197 nucleocapsid antigen expression in the unimmunized and adjuvant alone groups. By contrast, 1 of 5 of the
198 RBD-scNP + Alum immunized animals and 2 of 5 of the immunogen alone immunized animals had low
199 level nucleocapsid antigen expression, and no viral antigen was detected in the RBD-scNP plus 3M-052-
200 AF + Alum or RBD-scNP plus 3M-052-AF immunized animals (***Figure 3E***). Therefore, the three
201 adjuvants conferred comparable protection against viral replication by day 4 post-challenge, with 3M-
202 052-AF and 3M-052-AF + Alum providing the best reduction in virus replication when adjuvanting
203 RBD-scNP.
204
205 **RBD-scNP and S2P-scNP induce both ADCC-mediating and neutralizing antibodies**
206 While 90% of neutralizing antibodies target the RBD, neutralizing antibodies can target other sites on
207 spike. Thus, we generated scNPs with NTD and S-2P and compared the antibody response elicited by
208 these ferritin nanoparticles to RBD-scNPs (***Figure 4A-B***). Cynomolgus macaques were immunized three

209 times with one of the scNPs formulated with 3M-052-AF + Alum. After three immunizations, Spike
210 binding, ACE2-blocking, and neutralizing antibody-blocking antibodies were observed in all three groups
211 (***Supplementary Figure 3A-C***). In the RBD-scNP and S2P-scNP immunized animals, neutralizing
212 antibodies against SARS-CoV-2 D614G pseudovirus were detected after the first dose and were boosted
213 after the second dose at week 6 (***Figure 4C***). However, NTD-scNP failed to elicit neutralizing antibodies
214 against either pseudovirus or live SARS-CoV-2 virus (***Figure 4C-D***). Importantly, S2P-scNP induced
215 comparable plasma neutralizing antibody titers compared to RBD-scNP against SARS-CoV-2 WA-1
216 strain and all eight variants we tested ($p > 0.05$; Wilcoxon rank sum exact test; ***Figure 4E***) suggesting the
217 RBD was the main domain targeted by neutralizing antibodies. Among the different variants, the Beta
218 variant showed the largest reduction in neutralization ID_{50} titer (5.0- to10.9-fold) (***Figure 4F***). To
219 examine other antibody functions, we examined plasma antibody binding to cell surface-expressed
220 SARS-CoV-2 spike and antibody-dependent cellular cytotoxicity (ADCC). Plasma antibodies induced by
221 three doses of RBD-scNP, NTD-scNP and S2P-scNP vaccination bound to SARS-CoV-2 spike on the
222 surface of transfected cells (***Supplementary Figure 3D***). In a CD107a degranulation-based ADCC assay
223 (***Supplementary Figure 3E***), plasma antibodies from all three scNP groups mediated CD107a
224 degranulation of human NK cells in the presence of both SARS-CoV-2 spike-transfected cells and SARS-
225 CoV-2-infected cells (***Supplementary Figure 3F***). Thus, while all three scNP vaccines induced
226 antibodies that mediate ADCC, only RBD-scNP- and S2P-scNP-immunized NHP generated neutralizing
227 antibodies.
228
229 **RBD-scNP, NTD-scNP, and S2P-scNP vaccines protect macaques against SARS-CoV-2 WA-1**
230 **challenge**
231 To determine NTD-scNP and S2P-scNP immunization conferred protection against SARS-CoV-2,
232 we challenged the immunized macaques with SARS-CoV-2 WA-1 strain via the intratracheal and
233 intranasal routes after the 3rd vaccination. Remarkably, all macaques that received RBD-scNP, NTD-scNP
234 or S2P-scNP were fully protected, showing undetectable or near-detection-limit E or N gene sgRNA

235 (***Figure 4G and Supplementary Figure 3G***). IHC staining of the lung tissues demonstrated high SARS-
236 CoV-2 nucleocapsid protein expression in the control animals, whereas no viral antigen was detected in
237 any of the scNP-immunized animals (***Figure 4H-I***). The sgRNA and histopathology data demonstrated
238 that three doses of NTD-scNP or S2P-scNP immunization provided the same *in vivo* protection as RBD-
239 scNP immunization, preventing SARS-CoV-2 infection in both lower and upper respiratory tracts.
240

241 **RBD-scNP, NTD-scNP and S2P-scNP as boosts for mRNA-LNP vaccine elicited various**
242 **neutralizing antibody responses**

243 We next accessed the efficacy of the RBD-scNP, NTD-scNP and S2P-scNP as boosts in macaques
244 that received two priming doses of mRNA vaccine. Cynomolgus macaques (n=5) were immunized twice
245 with 50 μg of S-2P-encoding, nucleoside-modified mRNA encapsulated in lipid nanoparticles (S-2P
246 mRNA-LNP), which phenocopies the Pfizer/BioNTech and the Moderna COVID-19 vaccines.
247 Subsequently, macaques were boosted with RBD-, NTD- or S2P-scNPs (***Figure 4J***). Plasma antibody
248 binding patterns were similar among the three groups until animals received the scNP boosting
249 (***Supplementary Figure 4A***). Plasma antibodies targeting to ACE2-binding site and neutralizing epitopes
250 were detected after the scNP boosting with cross-reactive antibodies in the DH1047 blocking assay being
251 highest after RBD-scNP or S2P-NP boosting (***Supplementary Figure 4B-C***). BAL and nasal wash
252 mucosal ACE2-blocking and DH1047-blocking activities tended to be low in magnitude in macaques
253 primed with a Spike mRNA-LNP vaccine and boosted with RBD-scNP or S2P-scNP (***Supplementary***
254 ***Figure 4D-E***).

255 Serum neutralizing titers against the WA-1 strain pseudovirus were similar in the RBD-scNP-boosted
256 group (GMT ID_{50} = 10,912.1) and S2P-scNP-boosted group (GMT ID_{50} = 7799.9) (***Figure 4K***), while the
257 NTD-scNP-boosted group showed significantly lower titers (GMT ID_{50} = 3229.8; p = 0.027, exact
258 Wilcoxon test). The same differences were also observed in other major variants (***Figure 4K***). In addition,
259 in the RBD-scNP- and S2P-scNP-boosted groups, reduced ID_{50} titers were mostly seen for the Beta and
260 Gamma variants, whereas in the NTD-scNP-boosted group, Alpha, Beta, Gamma, Delta, Iota and Kappa

261 variants all showed >5-fold reduction of ID_{50} titers (***Figure 4L***). Thus, NTD-scNP was an inferior boost
262 of the S-2P mRNA-LNP vaccine compared to RBD- or S2P-scNPs.
263
264 **Protection of mRNA-LNP-primed and scNP-boosted macaques from SARS-CoV-2 challenge**
265 Macaques that received mRNA-LNP prime and scNP boost were challenged with SARS-CoV-2 WA-
266 1 strain after the RBD-scNP, NTD-scNP or S2P-scNP boosting. Four of five RBD-scNP-boosted
267 monkeys and four of five of the S2P-scNP-boosted monkeys were completely protected from SARS-
268 CoV-2 infection, showing no detectable E or N gene sgRNA in either BAL or nasal swab samples
269 (***Figure 4M and Supplementary Figure 4F***). However, in the NTD-scNP boost group, N gene sgRNA
270 was detected in BAL from three of five animals and in nasal swab samples from two of five animals
271 (***Figure 4M***). Macaques that received mRNA-LNP prime and RBD-scNP boost had the lowest extent of
272 lung inflammation, although the reduction in inflammation score did not reach statistical significance
273 (***Figure 4N***). In addition, no viral antigen was observed in lung tissues from either of the immunized
274 groups as indicated by IHC staining for SARS-CoV-2 N protein (***Figure 4O***). These data demonstrated
275 that RBD- and S2P-scNPs but not the NTD-scNPs, could serve as effective boosting immunogens
276 following mRNA-LNP vaccination.
277
278 **DISCUSSION**
279 In this study, the SARS-CoV-2 RBD has maintained conserved neutralizing epitopes among Beta,
280 Delta and Omicron variants, despite the up to 15 amino acid changes for the omicron variant relative to
281 the WA-1 strain. Given the neutralization titers that have protected macaques in challenge studies, we
282 speculate the RBD-scNP vaccine would protect against Omicron challenge with similar efficacy as shown
283 here for the Beta variant. While SARS-CoV-2 continues to mutate during the ongoing pandemic, there are
284 conserved RBD sites among the SARS-COV-2 variants. This result is supported by studies with a SARS-
285 CoV-2 virus where 20 naturally occurring mutations were introduced into the spike protein, but the
286 resultant virus was still sensitive to vaccine-induced polyclonal antibody responses (Schmidt et al., 2021).

287 For present and future coverage of SARS-CoV-2 variants, it will be critical to induce a polyclonal
288 response that targets conserved sites on the RBD. Monoclonal antibodies such as S2x259, S2K146
289 (Cameroni et al., 2021), DH1047 (Li *et al.*, 2021a; Martinez *et al.*, 2021a) or S309 (Pinto et al., 2020)
290 have defined these key conserved sites upon which vaccines can be designed.

291 Our studies with NTD-scNP immunization demonstrated neutralizing antibodies may not be the only
292 mediators of protection. While the RBD subunit has been shown to protect against SARS-CoV-2
293 challenge in animal models (Dai et al., 2020; Francica et al., 2021; Pino et al., 2021; Saunders *et al.*,
294 2021; Yang et al., 2020), the NTD is also an immunodominant region for neutralizing antibodies (Cerutti
295 et al., 2021; Chi et al., 2020; Li *et al.*, 2021a; Martinez et al., 2021b; McCallum et al., 2021; Voysey et
296 al., 2021). However, NTD is the site of multiple mutations and NTD antibody neutralization is, in
297 general, less potent than RBD antibodies. Here, no or minimal neutralizing antibody was detected in
298 NTD-scNP vaccinated monkeys, yet they were fully protected from WA-1 challenge. One hypothesis for
299 this result is that non-neutralizing antibodies induced by NTD-scNP protect against SARS-CoV-2. Serum
300 from the NTD-scNP group did have ADCC activity, suggesting that non-neutralizing Fc receptor-
301 mediated antibody activities could have been involved in protection. In this regard, we previously found
302 that a non-neutralizing NTD antibody DH1052 provided partial protection after infusion into mice and
303 non-human primates (Li *et al.*, 2021a). Moreover, we found that boosting with RBD-scNP or S2P-scNP
304 after S2P mRNA-LNPs priming afforded complete protection for monkeys after WA-1 challenge, while
305 NTD-scNP boosting of S2P mRNA-LNPs priming led to incomplete protection. The mechanism of this
306 finding is currently under investigation.

307 Finally, adjuvants play essential roles in vaccine formulation to elicit strong protective immune
308 responses (Coffman et al., 2010) and Alum is used in many currently approved vaccines (HogenEsch et
309 al., 2018). Thus, it was encouraging to see that the RBD-NP vaccine was protective in NHPs when
310 adsorbed to Alum. Compared to Alum, 3M-052-AF + Alum demonstrated superior capacities to elicit
311 neutralizing antibodies against SARS-CoV-2 WA-1 live virus when formulated with SARS-CoV-2 RBD
312 trimer in mice but not in rhesus macaques (Routhu et al., 2021). In addition, 3M-052-adjuvanted gp140

313 Env vaccine augmented neutralizing antibodies against tier 1A HIV-1 pseudovirus in rhesus macaques
314 (Kasturi et al., 2020). 3M-052-AF and 3M-052-AF + Alum are both in clinical testing for HIV-1 vaccines
315 (NCT04915768 and NCT04177355). Here we found that 3M-052-AF-adjuvanted vaccine induced not
316 only superior systemic and mucosal antibody responses, but also higher titers of neutralizing antibodies
317 than 3M-052-AF + Alum-adjuvanted vaccine, demonstrating that 3M-052-AF in the absence of Alum is
318 an optimal adjuvant for scNP. One explanation for this difference could be antagonism between Th1-
319 based immune pathways induced by 3M-052 (Smirnov et al., 2011) and Th2-based pathways induced by
320 Alum (Marrack et al., 2009). Another potential explanation is that physicochemical considerations such as
321 particle size or adsorption interactions between Alum and the RBD-scNP antigen and/or 3M-052-AF are
322 impacting vaccine biodistribution, presentation, or cellular processing, thus affecting downstream
323 immune responses. Such interactions are antigen-dependent (Fox et al., 2016), highlighting the
324 importance of optimizing adjuvant formulation for each unique antigen (Fox et al., 2013; HogenEsch *et*
325 *al.*, 2018). Coronavirus vaccines formulated with Alum have been reported to be associated with
326 enhanced lung inflammation, particularly with killed vaccines (Arvin et al., 2020; Haynes et al., 2020).
327 However, it is important to note that no enhancement of lung inflammation or virus replication was seen
328 with RBD-scNP/Alum formulations. The RBD-scNP + 3M-052-AF group exhibited the highest
329 neutralizing antibody titers and was the only group showing reduced severity of lung inflammation. That
330 Alum alone protected monkeys after immunization with RBD-scNPs raises the possibility of use in
331 pediatric populations.
332 Our study has several limitations. First, our study did not evaluate the durability of vaccine-induced
333 immune responses and protection against SARS-CoV-2 variants. Second, we did not set up longer time
334 intervals between the second and the third booster vaccination, to mimic 4-6 month boosting interval in
335 humans. Lastly, we challenged the animals with WA-1 strain, the Beta variant and the Delta variant;
336 future *in vivo* protection studies will be required upon availability of viral stocks of other SARS-CoV-2
337 variants such as the Omicron variant.

338 Thus, our study demonstrates that scNP vaccines with SARS-CoV-2 spike or spike subunits confer
339 potent protection in NHPs against WA-1, Beta and Delta variants, and that they induce neutralizing
340 antibodies to all SARS-CoV-2 variants tested *in vitro*. These findings have important implications for
341 development of the next generation of COVID-19 vaccines.
342
343
344 **MATERIALS AND METHODS**
345 **Animals and immunizations**
346 The study protocol and all veterinarian procedures were approved by the Bioqual IACUC per a
347 memorandum of understanding with the Duke IACUC, and were performed based on standard operating
348 procedures. Macaques studied were housed and maintained in an Association for Assessment and
349 Accreditation of Laboratory Animal Care-accredited institution in accordance with the principles of the
350 National Institutes of Health. All studies were carried out in strict accordance with the recommendations
351 in the Guide for the Care and Use of Laboratory Animals of the National Institutes of Health in
352 BIOQUAL (Rockville, MD). BIOQUAL is fully accredited by AAALAC and through OLAW, Assurance
353 Number A-3086. All physical procedures associated with this work were done under anesthesia to
354 minimize pain and distress in accordance with the recommendations of the Weatherall report, "The use of
355 non-human primates in research." Teklad 5038 Primate Diet was provided once daily by animal size and
356 weight. The diet was supplemented with fresh fruit and vegetables. Fresh water was given ad libitum. All
357 monkeys were maintained in accordance with the Guide for the Care and Use of Laboratory Animals.
358 Cynomolgus macaques were on average 8-9 years old and ranged from 2.75 to 8 kg in body weight.
359 Male and female macaques per group were balanced when availability permitted. Studies were performed
360 unblinded. The RBD-scNP, NTD-scNP and S2P-scNP immunogens were formulated with adjuvants as
361 previously described (Fox *et al.*, 2016) and given intramuscularly in the right and left quadriceps. In the
362 first study, cynomolgus macaques (n=5) were immunized for three times with 100 μg of RBD-scNP,
363 NTD-scNP and S2P-scNP adjuvanted with 5 μg of 3M-052 aqueous formulation admixed with 500 μg of

364 alum in PBS. In the second study, cynomolgus macaques (n=5) were were immunized twice with 50 μg
365 of S-2P mRNA-LNP (encoding the transmembrane spike protein stabilized with K986P and V987P
366 mutations) and boosted once with 100 μg of RBD-scNP, NTD-scNP and S2P-scNP adjuvanted with 5 μg
367 of 3M-052 aqueous formulation admixed with 500 μg of alum in PBS. In the third study, cynomolgus
368 macaques were immunized for twice with 100 μg of RBD-scNP or recombinant soluble RBD with 5 μg of
369 3M-052 aqueous formulation admixed with 500 μg of alum in PBS. In the fourth study, macaques were
370 divided into 8 groups (n=5 per group) as following: 1) control group: no immunization; 2) immunogen
371 alone group: 100 μg of RBD-scNP; 3) RBD-scNP + 3M-052-Alum group: 100 μg of RBD-scNP + 5 μg
372 of 3M-052 in aqueous formulation + 500 μg of Alum (i.e. aluminum ion); 4) 3M-052-Alum alone group:
373 5 μg of 3M-052 in aqueous formulation + 500 μg of Alum; 5) RBD-scNP + Alum group: 100 μg of RBD-
374 scNP + 500 μg of Alum; 6) Alum alone group: 500 μg of Alum; 7) RBD-scNP + 3M-052-AF group: 100
375 μg of RBD-scNP + 5 μg of 3M-052 in aqueous formulation; 8) 3M-052-AF alone group: 5 μg of 3M-052
376 in aqueous formulation.
377
378 **SARS-CoV-2 viral challenge**
379 For SARS-CoV-2 challenge, 10^5 plaque-forming units (PFU) of SARS-CoV-2 virus Isolate USA-
380 WA1/2020 (~10^6 TCID50) were diluted in 4 mL and were given by 1 mL intranasally and 3 mL
381 intratracheally on Day 0. Biospecimens, including nasal swabs, BAL, plasma, and serum samples, were
382 collected before immunization, after every immunization, before challenge, 2 days post-challenge and 4
383 days post-challenge. Animals were necropsied on Day 4 post-challenge, and lungs were collected for
384 histopathology and immunohistochemistry (IHC) analysis.
385
386 **Recombinant protein production**
387 The coronavirus ectodomain proteins were produced and purified as previously described (Li *et al.*,
388 2021a; Saunders *et al.*, 2021; Wrapp et al., 2020; Zhou et al., 2020). S-2P was stabilized by the
389 introduction of 2 prolines at amino acid positions 986 and 987. Plasmids encoding SARS-CoV-2 and

390 other coronavirus S-2P (Genscript) were transiently transfected in FreeStyle 293 cells (Thermo Fisher)
391 using Turbo293 (SpeedBiosystems) or 293Fectin (ThermoFisher). All cells were tested monthly for
392 mycoplasma. The constructs contained an HRV 3C-cleavable C-terminal twinStrepTagII-8×His tag. On
393 day 6, cell-free culture supernatant was generated by centrifugation of the culture and filtering through a
394 0.8-µm filter. Protein was purified from filtered cell culture supernatants by StrepTactin resin (IBA) and
395 by size-exclusion chromatography using Superose 6 column (GE Healthcare) in 10 mM Tris pH8,150
396 mM NaCl or 2 mM Tris pH 8, 200 mM NaCl, 0.02% NaN_3. ACE2-Fc was expressed by transient
397 transfection of Freestyle 293-F cells. ACE2-Fc was purified from cell culture supernatant by HiTrap
398 protein A column chromatography and Superdex200 size-exclusion chromatography in 10 mM Tris
399 pH8,150 mM NaCl. SARS-CoV-2 RBD and NTD were produced as previously described (Saunders *et*
400 *al.*, 2021; Zhou *et al.*, 2020).
401 RBD-scNP, NTD-scNP, and S2P-scNP were produced by conjugating SARS-CoV-2 RBD to *H.*
402 *pylori* ferritin nanoparticles using Sortase A as previously described (Saunders *et al.*, 2021). Briefly,
403 SARS-CoV-2 Wuhan strain RBD, NTD or S-2P (with a C-terminal foldon trimerization motif) was
404 expressed with a sortase A donor sequence LPETGG encoded at its C terminus. C-terminal to the sortase
405 A donor sequence was an HRV-3C cleavage site, 8×His tag and a twin StrepTagII (IBA). The proteins
406 were expressed in Freestyle 293 cells and purified by StrepTactin affinity chromatography and Superdex
407 200 size-exclusion chromatography. *Helicobacter pylori* ferritin particles were expressed with a
408 pentaglycine sortase A acceptor sequence encoded at its N terminus of each subunit. For affinity
409 purification of ferritin particles, 6×His tags were appended C-terminal to a HRV3C cleavage site. Ferritin
410 particles with a sortase A N-terminal tag were buffer exchanged into 50 mM Tris, 150 mM NaCl, 5 mM
411 $CaCl_2$, pH 7.5. Then 180 µM SARS-CoV-2 RBD was mixed with 120 µM of ferritin subunits and
412 incubated with 100 µM of sortase A overnight at room temperature. Following incubation, conjugated
413 particles were isolated from free ferritin or free RBD/NTD/S-2P by size-exclusion chromatography using
414 a Superose 6 16/60 column.
415

416 **mRNA-LNP vaccine production**

417 The S-2P mRNA was designed based on the SARS-CoV-2 spike (S) protein sequence (Wuhan-Hu-1)
418 and encoded the full-length S with K986P and V987P amino acid substitutions. Production of the mRNA
419 was performed as described earlier (Freyn et al., 2021; Freyn et al., 2020). Briefly, the codon-optimized
420 S-2P gene was synthesized (Genscript) and cloned into an mRNA production plasmid. A T7-driven in
421 vitro transcription reaction (Megascript, Ambion) using linearized plasmid template was performed to
422 generate mRNA with 101 nucleotide long poly(A) tail. Capping of the mRNA was performed in concert
423 with transcription through addition of a trinucleotide cap1 analog, CleanCap (TriLink) and m1Ψ-5'-
424 triphosphate (TriLink) was incorporated into the reaction instead of UTP. Cellulose-based purification of
425 S-2P mRNA was performed as described (Baiersdorfer et al., 2019). The S-2P mRNA was then tested on
426 an agarose gel before storing at -20°C. The cellulose-purified m1Ψ-containing S-2P mRNA was
427 encapsulated in LNPs using a self-assembly process as previously described wherein an ethanolic lipid
428 mixture of ionizable cationic lipid, phosphatidylcholine, cholesterol and polyethylene glycol-lipid was
429 rapidly mixed with an aqueous solution containing mRNA at acidic pH (Maier et al., 2013). The RNA-
430 loaded particles were characterized and subsequently stored at 80 °C at a concentration of 1 mg/ml.
431

432 **Antibody Binding ELISA**

433 For binding ELISA, 384-well ELISA plates were coated with 2 µg/mL of antigens in 0.1 M sodium
434 bicarbonate overnight at 4°C. Plates were washed with PBS + 0.05% Tween 20 and blocked with blocked
435 with assay diluent (PBS containing 4% (w/v) whey protein, 15% Normal Goat Serum, 0.5% Tween-20,
436 and 0.05% Sodium Azide) at room temperature for 1 hour. Plasma or mucosal fluid were serially diluted
437 threefold in superblock starting at a 1:30 dilution. Nasal fluid was started from neat, whereas BAL fluid
438 was concentrated ten-fold. To concentrate BAL, individual BAL aliquots from the same macaque and
439 same time point were pooled in 3-kDa MWCO ultrafiltration tubes (Sartorious, catalog # VS2091).
440 Pooled BAL was concentrated by centrifugation at 3,500 rpm for 30 min or until volume was reduced by
441 a factor of 10. The pool was then aliquoted and frozen at −80 °C until its use in an assay. Serially diluted

442 samples were added and incubated for 1 hour, followed by washing with PBS-0.1% Tween 20. HRP-
443 conjugated goat anti-human IgG secondary Ab (SouthernBiotech, catalog# 2040-05) was diluted to
444 1:10,000 and incubated at room temperature for 1 hour. These plates were washed four times and
445 developed with tetramethylbenzidine substrate (SureBlue Reserve- KPL). The reaction was stopped with
446 1 M HCl, and optical density at 450 nm (OD_{450}) was determined.
447
448 **ACE2 and neutralizing antibody blocking assay**
449 ELISA plates were coated as stated above with 2 µg/mL recombinant ACE-2 protein or neutralizing
450 antibodies, then washed and blocked with 3% BSA in 1x PBS. While assay plates blocked, plasma or
451 mucosal samples were diluted as stated above, only in 1% BSA with 0.05% Tween-20. In a separate
452 dilution plate spike-2P protein was mixed with the antibodies at a final concentration equal to the EC50 at
453 which spike binds to ACE-2 protein. The mixture was incubated at room temperature for 1 hour. Blocked
454 assay plates were then washed and the antibody-spike mixture was added to the assay plates for a period
455 of 1 hour at room temperature. Plates were washed and a polyclonal rabbit serum against the same spike
456 protein (nCoV-1 nCoV-2P.293F) was added for 1 hour, washed and detected with goat anti rabbit-HRP
457 (Abcam catalog # ab97080) followed by TMB substrate. The extent to which antibodies were able to
458 block the binding spike protein to ACE-2 or neutralizing antibodies was determined by comparing the OD
459 of antibody samples at 450 nm to the OD of samples containing spike protein only with no antibody. The
460 following formula was used to calculate percent blocking: blocking% = (100 - (OD sample/OD of spike
461 only)*100).
462
463 **Pseudotyped SARS-CoV-2 neutralization assay**
464 Neutralization of SARS-CoV-2 Spike-pseudotyped virus was performed by adopting an infection
465 assay described previously (Korber et al., 2020) with lentiviral vectors and infection in 293T/ACE2.MF
466 (the cell line was kindly provided by Drs. Mike Farzan and Huihui Mu at Scripps). Cells were maintained
467 in DMEM containing 10% FBS and 50 µg/ml gentamicin. An expression plasmid encoding codon-

468 optimized full-length spike of the Wuhan-1 strain (VRC7480), was provided by Drs. Barney Graham and
469 Kizzmekia Corbett at the Vaccine Research Center, National Institutes of Health (USA). Mutations were
470 introduced into VRC7480 either by site-directed mutagenesis using the QuikChange Lightning Site-
471 Directed Mutagenesis Kit from Agilent Technologies (Catalog # 210518), or were created by spike gene
472 synthesized by GenScript using the spike sequence in VRC7480 as template. All mutations were
473 confirmed by full-length spike gene sequencing by Sanger Sequencing, using Sequencher and SnapGene
474 for sequence analyses. D614G spike mutation: D614G; Alpha (B.1.1.7) spike mutations: Δ69-70, Δ144,
475 N501Y, A570D, D614G, P681H, T716I, S982A, D1118H; Beta (B.1.351) spike mutations: L18F, D80A,
476 D215G, Δ242-244, R246I, K417N, E484K, N501Y, D614G, A701V; Delta (B.1.617 AY.3) spike
477 mutations: T19R, G142D, Δ156-157, R158G, L452R, T478K, D614G, P681R, D950N; Epsilon (B.1.429)
478 spike mutations: S13I, W152C, L452R, D614G; Omicron (B.1.1.529) spike mutations: A67V, Δ69-70,
479 T95I, G142D, Δ143-145, Δ211, L212I, +214EPE, G339D, S371L, S373P, S375F, K417N, N440K,
480 G446S, S477N, T478K, E484A, Q493R, G496S, Q498R, N501Y, Y505H, T547K, D614G, H655Y,
481 N679K, P681H, N764K, D796Y, N856K, Q954H, N969K, L981F. Pseudovirions were produced in HEK
482 293T/17 cells (ATCC cat. no. CRL-11268) by transfection using Fugene 6 (Promega, Catalog #E2692).
483 Pseudovirions for 293T/ACE2 infection were produced by co-transfection with a lentiviral backbone
484 (pCMV ΔR8.2) and firefly luciferase reporter gene (pHR' CMV Luc) (Naldini et al., 1996). Culture
485 supernatants from transfections were clarified of cells by low-speed centrifugation and filtration (0.45 µm
486 filter) and stored in 1 ml aliquots at -80 °C. A pre-titrated dose of virus was incubated with 8 serial 3-fold
487 or 5-fold dilutions of mAbs in duplicate in a total volume of 150 µl for 1 hr at 37 °C in 96-well flat-
488 bottom poly-L-lysine-coated culture plates (Corning Biocoat). Cells were suspended using TrypLE
489 express enzyme solution (Thermo Fisher Scientific) and immediately added to all wells (10,000 cells in
490 100 µL of growth medium per well). One set of 8 control wells received cells + virus (virus control) and
491 another set of 8 wells received cells only (background control). After 66-72 hrs of incubation, medium
492 was removed by gentle aspiration and 30 µL of Promega 1x lysis buffer was added to all wells. After a

493 10-minute incubation at room temperature, 100 µl of Bright-Glo luciferase reagent was added to all wells.
494 After 1-2 minutes, 110 µl of the cell lysate was transferred to a black/white plate (Perkin-Elmer).
495 Luminescence was measured using a PerkinElmer Life Sciences, Model Victor2 luminometer.
496 Neutralization titers are the mAb concentration (IC50/IC80) at which relative luminescence units (RLU)
497 were reduced by 50% and 80% compared to virus control wells after subtraction of background RLUs.
498 Negative neutralization values are indicative of infection-enhancement. Maximum percent inhibition
499 (MPI) is the reduction in RLU at the highest mAb concentration tested.
500 Another protocol was used to test plasma neutralization against pseudoviruses of SARS-CoV-2 WA-
501 1 strain and variants. Human codon-optimized cDNA encoding SARS-CoV-2 spike glycoproteins of
502 various strains were synthesized by GenScript and cloned into eukaryotic cell expression vector pcDNA
503 3.1 between the BamHI and XhoI sites. Pseudovirions were produced by co-transfection of Lenti-X 293T
504 cells with psPAX2(gag/pol), pTrip-luc lentiviral vector and pcDNA 3.1 SARS-CoV-2-spike-deltaC19,
505 using Lipofectamine 3000. The supernatants were collected at 48 h after transfection and filtered through
506 0.45-µm membranes and titrated using HEK293T cells that express ACE2 and TMPRSS2 protein (293T-
507 ACE2-TMPRSS2 cells). For the neutralization assay, 50 µl of SARS-CoV-2 spike pseudovirions were
508 pre-incubated with an equal volume of medium containing serum at varying dilutions at room temperature
509 for 1 h, then virus-antibody mixtures were added to 293T-ACE2-TMPRSS2 cells in a 96-well plate. After
510 a 3-h incubation, the inoculum was replaced with fresh medium. Cells were lysed 24 h later, and
511 luciferase activity was measured using luciferin. Controls included cell-only control, virus without any
512 antibody control and positive control sera. Neutralization titres are the serum dilution (ID50 or ID80) at
513 which relative luminescence units (RLU) were reduced by 50% or 80%, respectively, compared to virus
514 control wells after subtraction of background RLUs.
515
516 **Live SARS-CoV-2 neutralization assays**
517 The SARS-CoV-2 virus (Isolate USA-WA1/2020, NR-52281) was deposited by the Centers for
518 Disease Control and Prevention and obtained through BEI Resources, NIAID, NIH. SARS-CoV-2 Plaque

519 Reduction Neutralization Test (PRNT) were performed in the Duke Regional Biocontaiment Laboratory
520 BSL3 (Durham, NC) as previously described with virus-specific modifications (Berry et al., 2004).
521 Briefly, two-fold dilutions of plasma samples were incubated with 50 PFU SARS-CoV-2 virus (Isolate
522 USA-WA1/2020, NR-52281) for 1 hour. The antibody/virus mixture is used to inoculate Vero E6 cells in
523 a standard plaque assay (Coleman and Frieman, 2015; Kint et al., 2015). Briefly, infected cultures are
524 incubated at 37°C, 5% CO2 for 1 hour. At the end of the incubation, 1 mL of a viscous overlay (1:1 2x
525 DMEM and 1.2% methylcellulose) is added to each well. Plates are incubated for 4 days. After fixation,
526 staining and washing, plates are dried and plaques from each dilution of each sample are counted. Data
527 are reported as the concentration at which 50% of input virus is neutralized. A known neutralizing control
528 antibody is included in each batch run (Clone D001; SINO, CAT# 40150-D001). GraphPad Prism was
529 used to determine IC/EC_{50} values.
530
531 **Spike protein-expressing cell antibody binding assay**
532 The cell antibody binding assay was performed as previously described (Pino et al., 2021). Briefly,
533 target cells were derived by transfection with plasmids designed to express the SARS-CoV-2 D614 Spike
534 protein with a c-terminus flag tag (kindly provided by Dr. Farzan, Addgene plasmid no. 156420 (Zhang et
535 al., 2020)). Cells not transfected with any plasmid (mock transfected) were used as a negative control
536 condition. After resuspension, washing and counting, $1x10^5$ Spike-transfected target cells were dispensed
537 into 96-well V-bottom plates and incubated with six serial dilutions of human plasma from infected
538 participants starting at 1:50 dilution. Mock transfected cells were used as a negative infection control.
539 After 30 minutes incubation at 37°C, cells are washed twice with 250 µL/well of PBS, stained with vital
540 dye (Live/Dead Far Red Dead Cell Stain, Invitrogen) to exclude nonviable cells from subsequent analysis,
541 washed with Wash Buffer (1%FBS-PBS; WB), permeabilized with CytoFix/CytoPerm (BD Biosciences),
542 and stained with 1.25 µg/mL anti-human IgG Fc-PE/Cy7 (Clone HP6017; Biolegend) and 5 µg/mL anti-
543 flag-FITC (clone M2; Sigma Aldrich) in the dark for 20 minutes at room temperature. After three washes
544 with Perm Wash (BD Biosciences), the cells were resuspended in 125 µL PBS-1% paraformaldehyde.

545 Samples were acquired within 24 h using a BD Fortessa cytometer and a High Throughput Sampler
546 (HTS, BD Biosciences). Data analysis was performed using FlowJo 10 software (BD Biosciences). A
547 minimum of 50,000 total events were acquired for each analysis. Gates were set to include singlet, live,
548 flag+ and IgG+ events. All final data represent specific binding, determined by subtraction of non-
549 specific binding observed in assays performed with mock-transfected cells.
550
551 **Antibody-dependent NK cell degranulation assay**
552 Cell-surface expression of CD107a was used as a marker for NK cell degranulation, a prerequisite
553 process for ADCC (Ferrari et al., 2011), was performed as previously described (Pino et al., 2021).
554 Briefly, target cells were either Vero E6 cells after a 2 day-infection with SARS-CoV-2 USA-WA1/2020
555 or 293T cells 2-days post transfection with a SARS-CoV-2 S protein (D614) expression plasmid. NK
556 cells were purified from peripheral blood of a healthy human volunteer by negative selection (Miltenyi
557 Biotech), and were incubated with target cells at a 1:1 ratio in the presence of diluted plasma or
558 monoclonal antibodies, Brefeldin A (GolgiPlug, 1 µl/ml, BD Biosciences), monensin (GolgiStop,
559 4µl/6mL, BD Biosciences), and anti-CD107a-FITC (BD Biosciences, clone H4A3) in 96-well flat bottom
560 plates for 6 hours at 37ºC in a humidified 5% CO2 incubator. NK cells were then recovered and stained
561 for viability prior to staining with CD56-PECy7 (BD Biosciences, clone NCAM16.2), CD16-PacBlue
562 (BD Biosciences, clone 3G8), and CD69-BV785 (Biolegend, Clone FN50). Flow cytometry data analysis
563 was performed using FlowJo software (v10.8.0). Data is reported as the % of CD107A+ live NK cells
564 (gates included singlets, lymphocytes, aqua blue-, CD56+ and/or CD16+, CD107A+). All final data
565 represent specific activity, determined by subtraction of non-specific activity observed in assays
566 performed with mock-infected cells and in absence of antibodies.
567
568 **Viral RNA Extraction and Subgenomic mRNA quantification**
569 SARS-CoV-2 E gene and N gene subgenomic mRNA (sgRNA) was measured by a one-step RT-
570 qPCR adapted from previously described methods (Wolfel et al., 2020; Yu et al., 2020). To generate

571 standard curves, a SARS-CoV-2 E gene sgRNA sequence, including the 5'UTR leader sequence,
572 transcriptional regulatory sequence (TRS), and the first 228 bp of E gene, was cloned into a pcDNA3.1
573 plasmid. For generating SARS-CoV-2 N gene sgRNA, the E gene was replaced with the first 227 bp of N
574 gene. The recombinant pcDNA3.1 plasmid was linearized, transcribed using MEGAscript T7
575 Transcription Kit (ThermoFisher, catalog # AM1334), and purified with MEGAclear Transcription
576 Clean-Up Kit (ThermoFisher, catalog # AM1908). The purified RNA products were quantified on
577 Nanodrop, serial diluted, and aliquoted as E sgRNA or N sgRNA standards.
578 A QIAsymphony SP (Qiagen, Hilden, Germany) automated sample preparation platform along with a
579 virus/pathogen DSP midi kit. RNA extracted from animal samples or standards were then measured in
580 Taqman custom gene expression assays (ThermoFisher). For these assays we used TaqMan Fast Virus 1-
581 Step Master Mix (ThermoFisher, catalog # 4444432) and custom primers/probes targeting the E gene
582 sgRNA (forward primer: 5' CGA TCT CTT GTA GAT CTG TTC TCE 3'; reverse primer: 5' ATA TTG
583 CAG CAG TAC GCA CAC A 3'; probe: 5' FAM-ACA CTA GCC ATC CTT ACT GCG CTT CG-
584 BHQ1 3') or the N gene sgRNA (forward primer: 5' CGA TCT CTT GTA GAT CTG TTC TC 3';
585 reverse primer: 5' GGT GAA CCA AGA CGC AGT AT 3'; probe: 5' FAM-TAA CCA GAA TGG AGA
586 ACG CAG TGG G-BHQ1 3'). RT-qPCR reactions were carried out on CFX384 Touch Real-Time PCR
587 System (Bio-Rad) using a program below: reverse transcription at 50°C for 5 minutes, initial denaturation
588 at 95°C for 20 seconds, then 40 cycles of denaturation-annealing-extension at 95°C for 15 seconds and
589 60°C for 30 seconds. Standard curves were used to calculate E or N sgRNA in copies per ml; the limit of
590 detections (LOD) for both E and N sgRNA assays were 12.5 copies per reaction or 150 copies per mL of
591 BAL/nasal swab.
592
593 **Histopathology**
594 Lung specimen from nonhuman primates were fixed in 10% neutral buffered formalin, processed,
595 and blocked in paraffin for histological analysis. All samples were sectioned at 5 μm and stained with
596 hematoxylin-eosin (H&E) for routine histopathology. Sections were examined under light microscopy

597 using an Olympus BX51 microscope and photographs were taken using an Olympus DP73 camera.
598 Samples were scored by a board-certified veterinary pathologist in a blinded manner. The representative
599 images are to characterize the types and arrangement of inflammatory cells, while the scores show the
600 relative severity of the tissue section.
601
602 **Immunohistochemistry (IHC)**
603 Staining for SARS-CoV-2 antigen was achieved on the Bond RX automated system with the
604 Polymer Define Detection System (Leica) used per manufacturer's protocol. Tissue sections were
605 dewaxed with Bond Dewaxing Solution (Leica) at 72°C for 30 min then subsequently rehydrated with
606 graded alcohol washes and 1x Immuno Wash (StatLab). Heat-induced epitope retrieval (HIER) was
607 performed using Epitope Retrieval Solution 1 (Leica), heated to 100°C for 20 minutes. A peroxide block
608 (Leica) was applied for 5 min to quench endogenous peroxidase activity prior to applying the SARS-
609 CoV-2 antibody (1:2000, GeneTex, GTX135357). Antibodies were diluted in Background Reducing
610 Antibody Diluent (Agilent). The tissue was subsequently incubated with an anti-rabbit HRP polymer
611 (Leica) and colorized with 3,3'-Diaminobenzidine (DAB) chromogen for 10 min. Slides were
612 counterstained with hematoxylin.
613
614 **Negative-stain electron microscopy**
615 Samples diluted to 200 µg/ml with 5 g/dl Glycerol in HBS (20 mM HEPES, 150 mM NaCl pH
616 7.4) buffer containing 8 mM glutaraldehyde. After 5 min incubation, glutaraldehyde was quenched by
617 adding sufficient 1 M Tris stock, pH 7.4, to give 75 mM final Tris concentration and incubated for 5 min.
618 Quenched sample was applied to a glow-discharged carbon-coated EM grid for 10-12 second, then
619 blotted, and stained with 2 g/dL uranyl formate for 1 min, blotted and air-dried. Grids were examined on a
620 Philips EM420 electron microscope operating at 120 kV and nominal magnification of 82,000x, and
621 images were collected on a 4 Mpix CCD camera at 4 Å/pixel. Images were analyzed by 2D class averages
622 using standard protocols with Relion 3.0 (Zivanov et al., 2018). The Relion reference needs to be added to

623 the references. Also let us know which lot# you are shown in this manuscript so we can double check
624 whether images are collected with old or new camera. Since the magnification and Å/pixel is different.
625
626 **Mouse immunization and challenge**
627 Eleven-month-old female BALB/c mice were purchased from Envigo (#047) and were used for the
628 SARS-CoV, SARS-CoV-2 WA-1, SARS-CoV-2 B.1.351, and RsSHC014-CoV protection experiments.
629 The study was carried out in accordance with the recommendations for care and use of animals by the
630 Office of Laboratory Animal Welfare (OLAW), National Institutes of Health and the Institutional Animal
631 Care and Use Committee (IACUC) of University of North Carolina (UNC permit no. A-3410-01).
632 Animals were housed in groups of five and fed standard chow diets. Virus inoculations were performed
633 under anesthesia and all efforts were made to minimize animal suffering. Mice were intramuscularly
634 immunized with RBD-scNP formulated with 3M-052-AF + Alum or GLA-SE. For the SARS-CoV-2
635 WA-1 and RsSHC014 study, mice were immunized on week 0 and 2, and challenged on week 7. For the
636 SARS-CoV-2 B.1.351 and SARS-CoV-1 study, mice were immunized on week 0 and 4, and challenged
637 on week 6. All mice were anesthetized and infected intranasally with 1×10^4 PFU/ml of SARS-CoV
638 MA15, 1×10^4 PFU/ml of SARS-CoV-2 WA1- MA10 or B.1.351-MA10, 1×10^4 PFU/ml RsSHC014,
639 which have been described previously (Leist et al., 2020; Martinez *et al.*, 2021a; Martinez *et al.*, 2021b;
640 Menachery et al., 2015; Roberts et al., 2007). Mice were weighted daily and monitored for signs of
641 clinical disease, and selected groups were subjected to daily whole-body plethysmography. For all mouse
642 studies, groups of n=10 mice were included per arm of the study. Lung viral titers and weight loss were
643 measured from individual mice per group.
644
645 **Biocontainment and biosafety**
646 Studies were approved by the UNC Institutional Biosafety Committee approved by animal and
647 experimental protocols in the Baric laboratory. All work described here was performed with approved

648 standard operating procedures for SARS-CoV-2 in a biosafety level 3 (BSL-3) facility conforming to
649 requirements recommended in the Microbiological and Biomedical Laboratories, by the U.S. Department
650 of Health and Human Service, the U.S. Public Health Service, and the U.S. Center for Disease Control
651 and Prevention (CDC), and the National Institutes of Health (NIH).
652
653 **Statistics Analysis**
654 Data were plotted using Prism GraphPad 8.0. Wilcoxon rank sum exact test was performed to
655 compare differences between groups with p-value < 0.05 considered significant using SAS 9.4 (SAS
656 Institute, Cary, NC). The Benjamini-Hochberg correction (Benjamini and Hochberg, 1995) was used to
657 adjust the *p*-values for multiple comparisons.
658
659
660 **DATA AVAILABILITY**
661 The data that support the findings of this study are available from the corresponding authors upon
662 reasonable request.
663
664 **AUTHOR CONTRIBUTIONS**
665 D.L. performed RNA assays, analyzed the data and wrote the manuscript; D.R.M., A.S., and R.S.B.
666 performed or supervised the mouse challenge studies; L.L.S., M.B., W.E., A.N. performed monkey
667 studies and managed monkey samples; H.C., E.L. performed protein production; M.B., R.P. carried out
668 ELISA assays; T.H.O., G.D.S., D.C.M., A.E., H.G. and S.K. carried out neutralization assays; D.L.,
669 C.T.M., T.N.D., M.G., D.C.D. designed or performed subgenomic RNA assays; K.W.B., M.M., B.M.N.,
670 I.N.M. performed histopathology analysis; D.M., G.F., D.W.C., and S.S. performed staining and ADCC
671 assays; K.M. and R.J.E. performed negative staining EM; R.W.R. and Y.W. performed statistical
672 analyses; M.A.T. selected and provided adjuvant; C.B.F. formulated 3M-052 in alum; N.P. and D.W.
673 provided the mRNA-LNP vaccine; M.A.T. selected and provided adjuvant; C.B.F. formulated 3M-052;

674 M.G.L., H.A. and R.S. evaluated and supervised monkey studies; K.O.S. designed the antigens,
675 supervised the protein production, and edited the manuscript; B.F.H. designed and managed the study,
676 reviewed all data and wrote and edited the manuscript. All authors edited and approved the manuscript.
677

678 **COMPETING FINANCIAL INTERESTS**

679 B.F.H. and K.O.S. have filed US patents regarding the nanoparticle vaccine, M.A.T. and the 3M
680 company have US patents filed on 3M-052, and C.B.F. and IDRI have filed a patent on the formulation of
681 3M-052-AF and 3M-052-AF + Alum. The 3M company had no role in the execution of the study, data
682 collection or data interpretation. D.W. is named on US patents that describe the use of nucleoside-
683 modified mRNA as a platform to deliver therapeutic proteins. D.W. and N.P. are also named on a US
684 patent describing the use of nucleoside-modified mRNA in lipid nanoparticles as a vaccine platform. All
685 other authors declare no competing interests.
686

687 **ACKNOWLEDGEMENTS**

688 We thank Margaret Deyton, Victoria Gee-Lai, Nicole De Naeyer and Conor Anderson for technical
689 assistance. We thank Elizabeth Donahue, Cynthia Nagle and Kelly Soderberg for program management.
690 We thank John Harrison, Alex Granados, Adrienne Goode, Anthony Cook, Alan Dodson, Katelyn
691 Steingrebe, Bridget Bart, Laurent Pessaint, Alex VanRy, Daniel Valentin, Amanda Strasbaugh, and
692 Mehtap Cabus for assistance with macaque studies. This work was supported by funds from the State of
693 North Carolina with funds from the federal CARES Act; NIH, NIAID, DAIDS grant AI142596 (B.F.H.),
694 AI158571 (B.F.H.), UC6-AI058607, G20-AI167200 (G.D.S.); the Ting Tsung & Wei Fong Chao
695 Foundation (B.F.H.); Hanna H Gray Fellowship from the Howard Hughes Medical Institute and a
696 Postdoctoral Enrichment Award from the Burroughs Wellcome Fund (D.R.M.).
697

698 **REFERENCES**

699 Arvin, A.M., Fink, K., Schmid, M.A., Cathcart, A., Spreafico, R., Havenar-Daughton, C., Lanzavecchia,
700 A., Corti, D., and Virgin, H.W. (2020). A perspective on potential antibody-dependent enhancement of
701 SARS-CoV-2. Nature *584*, 353-363. 10.1038/s41586-020-2538-8.
702 Baden, L.R., El Sahly, H.M., Essink, B., Kotloff, K., Frey, S., Novak, R., Diemert, D., Spector, S.A.,
703 Rouphael, N., Creech, C.B., et al. (2021). Efficacy and Safety of the mRNA-1273 SARS-CoV-2 Vaccine.
704 N Engl J Med *384*, 403-416. 10.1056/NEJMoa2035389.
705 Baiersdorfer, M., Boros, G., Muramatsu, H., Mahiny, A., Vlatkovic, I., Sahin, U., and Kariko, K. (2019).
706 A Facile Method for the Removal of dsRNA Contaminant from In Vitro-Transcribed mRNA. Mol Ther
707 Nucleic Acids *15*, 26-35. 10.1016/j.omtn.2019.02.018.
708 Benjamini, Y., and Hochberg, Y. (1995). Controlling the False Discovery Rate: A Practical and Powerful
709 Approach to Multiple Testing. Journal of the Royal Statistical Society. Series B (Methodological) *57*,
710 289-300.
711 Berry, J.D., Jones, S., Drebot, M.A., Andonov, A., Sabara, M., Yuan, X.Y., Weingartl, H., Fernando, L.,
712 Marszal, P., Gren, J., et al. (2004). Development and characterisation of neutralising monoclonal antibody
713 to the SARS-coronavirus. J Virol Methods *120*, 87-96. 10.1016/j.jviromet.2004.04.009.
714 Cameroni, E., Bowen, J.E., Rosen, L.E., Saliba, C., Zepeda, S.K., Culap, K., Pinto, D., VanBlargan, L.A.,
715 De Marco, A., di Iulio, J., et al. (2021). Broadly neutralizing antibodies overcome SARS-CoV-2 Omicron
716 antigenic shift. Nature. 10.1038/s41586-021-04386-2.
717 Cerutti, G., Guo, Y., Zhou, T., Gorman, J., Lee, M., Rapp, M., Reddem, E.R., Yu, J., Bahna, F., Bimela,
718 J., et al. (2021). Potent SARS-CoV-2 neutralizing antibodies directed against spike N-terminal domain
719 target a single supersite. Cell Host Microbe. 10.1016/j.chom.2021.03.005.
720 Chaudhary, N., Weissman, D., and Whitehead, K.A. (2021). mRNA vaccines for infectious diseases:
721 principles, delivery and clinical translation. Nat Rev Drug Discov *20*, 817-838. 10.1038/s41573-021-
722 00283-5.

723 Chi, X., Yan, R., Zhang, J., Zhang, G., Zhang, Y., Hao, M., Zhang, Z., Fan, P., Dong, Y., Yang, Y., et al.
724 (2020). A potent neutralizing human antibody reveals the N-terminal domain of the Spike protein of
725 SARS-CoV-2 as a site of vulnerability. 10.1101/2020.05.08.083964.
726 Coffman, R.L., Sher, A., and Seder, R.A. (2010). Vaccine adjuvants: putting innate immunity to work.
727 Immunity *33*, 492-503. 10.1016/j.immuni.2010.10.002.
728 Coleman, C.M., and Frieman, M.B. (2015). Growth and Quantification of MERS-CoV Infection. Curr
729 Protoc Microbiol *37*, 15E 12 11-19. 10.1002/9780471729259.mc15e02s37.
730 Dai, L., Zheng, T., Xu, K., Han, Y., Xu, L., Huang, E., An, Y., Cheng, Y., Li, S., Liu, M., et al. (2020). A
731 Universal Design of Betacoronavirus Vaccines against COVID-19, MERS, and SARS. Cell *182*, 722-733
732 e711. 10.1016/j.cell.2020.06.035.
733 Fox, C.B., Kramer, R.M., Barnes, V.L., Dowling, Q.M., and Vedvick, T.S. (2013). Working together:
734 interactions between vaccine antigens and adjuvants. Ther Adv Vaccines *1*, 7-20.
735 10.1177/2051013613480144.
736 Fox, C.B., Orr, M.T., Van Hoeven, N., Parker, S.C., Mikasa, T.J., Phan, T., Beebe, E.A., Nana, G.I.,
737 Joshi, S.W., Tomai, M.A., et al. (2016). Adsorption of a synthetic TLR7/8 ligand to aluminum
738 oxyhydroxide for enhanced vaccine adjuvant activity: A formulation approach. J Control Release *244*, 98-
739 107. 10.1016/j.jconrel.2016.11.011.
740 Francica, J.R., Flynn, B.J., Foulds, K.E., Noe, A.T., Werner, A.P., Moore, I.N., Gagne, M., Johnston,
741 T.S., Tucker, C., Davis, R.L., et al. (2021). Protective antibodies elicited by SARS-CoV-2 spike protein
742 vaccination are boosted in the lung after challenge in nonhuman primates. Sci Transl Med *13*.
743 10.1126/scitranslmed.abi4547.
744 Freyn, A.W., Pine, M., Rosado, V.C., Benz, M., Muramatsu, H., Beattie, M., Tam, Y.K., Krammer, F.,
745 Palese, P., Nachbagauer, R., et al. (2021). Antigen modifications improve nucleoside-modified mRNA-
746 based influenza virus vaccines in mice. Mol Ther Methods Clin Dev *22*, 84-95.
747 10.1016/j.omtm.2021.06.003.

748 Freyn, A.W., Ramos da Silva, J., Rosado, V.C., Bliss, C.M., Pine, M., Mui, B.L., Tam, Y.K., Madden,
749 T.D., de Souza Ferreira, L.C., Weissman, D., et al. (2020). A Multi-Targeting, Nucleoside-Modified
750 mRNA Influenza Virus Vaccine Provides Broad Protection in Mice. Mol Ther *28*, 1569-1584.
751 10.1016/j.ymthe.2020.04.018.
752 Hastie, K.M., Li, H., Bedinger, D., Schendel, S.L., Dennison, S.M., Li, K., Rayaprolu, V., Yu, X., Mann,
753 C., Zandonatti, M., et al. (2021). Defining variant-resistant epitopes targeted by SARS-CoV-2 antibodies:
754 A global consortium study. Science *374*, 472-478. 10.1126/science.abh2315.
755 Haynes, B.F. (2021). A New Vaccine to Battle Covid-19. N Engl J Med *384*, 470-471.
756 10.1056/NEJMe2035557.
757 Haynes, B.F., Corey, L., Fernandes, P., Gilbert, P.B., Hotez, P.J., Rao, S., Santos, M.R., Schuitemaker,
758 H., Watson, M., and Arvin, A. (2020). Prospects for a safe COVID-19 vaccine. Sci Transl Med *12*.
759 10.1126/scitranslmed.abe0948.
760 HogenEsch, H., O'Hagan, D.T., and Fox, C.B. (2018). Optimizing the utilization of aluminum adjuvants
761 in vaccines: you might just get what you want. NPJ Vaccines *3*, 51. 10.1038/s41541-018-0089-x.
762 Kasturi, S.P., Rasheed, M.A.U., Havenar-Daughton, C., Pham, M., Legere, T., Sher, Z.J., Kovalenkov,
763 Y., Gumber, S., Huang, J.Y., Gottardo, R., et al. (2020). 3M-052, a synthetic TLR-7/8 agonist, induces
764 durable HIV-1 envelope-specific plasma cells and humoral immunity in nonhuman primates. Sci
765 Immunol *5*. 10.1126/sciimmunol.abb1025.
766 Kint, J., Maier, H.J., and Jagt, E. (2015). Quantification of infectious bronchitis coronavirus by titration in
767 vitro and in ovo. Methods Mol Biol *1282*, 89-98. 10.1007/978-1-4939-2438-7_9.
768 Korber, B., Fischer, W.M., Gnanakaran, S., Yoon, H., Theiler, J., Abfalterer, W., Hengartner, N., Giorgi,
769 E.E., Bhattacharya, T., Foley, B., et al. (2020). Tracking Changes in SARS-CoV-2 Spike: Evidence that
770 D614G Increases Infectivity of the COVID-19 Virus. Cell *182*, 812-827 e819.
771 10.1016/j.cell.2020.06.043.

772 Leist, S.R., Dinnon, K.H., 3rd, Schäfer, A., Tse, L.V., Okuda, K., Hou, Y.J., West, A., Edwards, C.E.,
773 Sanders, W., Fritch, E.J., et al. (2020). A Mouse-Adapted SARS-CoV-2 Induces Acute Lung Injury and
774 Mortality in Standard Laboratory Mice. Cell *183*, 1070-1085.e1012. 10.1016/j.cell.2020.09.050.
775 Levin, E.G., Lustig, Y., Cohen, C., Fluss, R., Indenbaum, V., Amit, S., Doolman, R., Asraf, K.,
776 Mendelson, E., Ziv, A., et al. (2021). Waning Immune Humoral Response to BNT162b2 Covid-19
777 Vaccine over 6 Months. N Engl J Med. 10.1056/NEJMoa2114583.
778 Li, D., Edwards, R.J., Manne, K., Martinez, D.R., Schafer, A., Alam, S.M., Wiehe, K., Lu, X., Parks, R.,
779 Sutherland, L.L., et al. (2021a). In vitro and in vivo functions of SARS-CoV-2 infection-enhancing and
780 neutralizing antibodies. Cell *184*, 4203-4219 e4232. 10.1016/j.cell.2021.06.021.
781 Li, D., Sempowski, G.D., Saunders, K.O., Acharya, P., and Haynes, B.F. (2021b). SARS-CoV-2
782 Neutralizing Antibodies for COVID-19 Prevention and Treatment. Annu Rev Med. 10.1146/annurev-
783 med-042420-113838.
784 Maier, M.A., Jayaraman, M., Matsuda, S., Liu, J., Barros, S., Querbes, W., Tam, Y.K., Ansell, S.M.,
785 Kumar, V., Qin, J., et al. (2013). Biodegradable lipids enabling rapidly eliminated lipid nanoparticles for
786 systemic delivery of RNAi therapeutics. Mol Ther *21*, 1570-1578. 10.1038/mt.2013.124.
787 Marrack, P., McKee, A.S., and Munks, M.W. (2009). Towards an understanding of the adjuvant action of
788 aluminium. Nat Rev Immunol *9*, 287-293. 10.1038/nri2510.
789 Martinez, D.R., Schafer, A., Gobeil, S., Li, D., De la Cruz, G., Parks, R., Lu, X., Barr, M., Stalls, V.,
790 Janowska, K., et al. (2021a). A broadly cross-reactive antibody neutralizes and protects against
791 sarbecovirus challenge in mice. Sci Transl Med, eabj7125. 10.1126/scitranslmed.abj7125.
792 Martinez, D.R., Schafer, A., Leist, S.R., De la Cruz, G., West, A., Atochina-Vasserman, E.N.,
793 Lindesmith, L.C., Pardi, N., Parks, R., Barr, M., et al. (2021b). Chimeric spike mRNA vaccines protect
794 against Sarbecovirus challenge in mice. Science *373*, 991-998. 10.1126/science.abi4506.
795 McCallum, M., De Marco, A., Lempp, F.A., Tortorici, M.A., Pinto, D., Walls, A.C., Beltramello, M.,
796 Chen, A., Liu, Z., Zatta, F., et al. (2021). N-terminal domain antigenic mapping reveals a site of
797 vulnerability for SARS-CoV-2. Cell. 10.1016/j.cell.2021.03.028.

798 Menachery, V.D., Yount, B.L., Jr., Debbink, K., Agnihothram, S., Gralinski, L.E., Plante, J.A., Graham,
799 R.L., Scobey, T., Ge, X.Y., Donaldson, E.F., et al. (2015). A SARS-like cluster of circulating bat
800 coronaviruses shows potential for human emergence. Nat Med *21*, 1508-1513. 10.1038/nm.3985.
801 Naldini, L., Blomer, U., Gage, F.H., Trono, D., and Verma, I.M. (1996). Efficient transfer, integration,
802 and sustained long-term expression of the transgene in adult rat brains injected with a lentiviral vector.
803 Proc Natl Acad Sci U S A *93*, 11382-11388. 10.1073/pnas.93.21.11382.
804 Pardi, N., Hogan, M.J., Porter, F.W., and Weissman, D. (2018). mRNA vaccines - a new era in
805 vaccinology. Nat Rev Drug Discov *17*, 261-279. 10.1038/nrd.2017.243.
806 Pardi, N., Hogan, M.J., and Weissman, D. (2020). Recent advances in mRNA vaccine technology. Curr
807 Opin Immunol *65*, 14-20. 10.1016/j.coi.2020.01.008.
808 Pino, M., Abid, T., Pereira Ribeiro, S., Edara, V.V., Floyd, K., Smith, J.C., Latif, M.B., Pacheco-Sanchez,
809 G., Dutta, D., Wang, S., et al. (2021). A yeast expressed RBD-based SARS-CoV-2 vaccine formulated
810 with 3M-052-alum adjuvant promotes protective efficacy in non-human primates. Sci Immunol *6*.
811 10.1126/sciimmunol.abh3634.
812 Pinto, D., Park, Y.J., Beltramello, M., Walls, A.C., Tortorici, M.A., Bianchi, S., Jaconi, S., Culap, K.,
813 Zatta, F., De Marco, A., et al. (2020). Cross-neutralization of SARS-CoV-2 by a human monoclonal
814 SARS-CoV antibody. Nature *583*, 290-295. 10.1038/s41586-020-2349-y.
815 Polack, F.P., Thomas, S.J., Kitchin, N., Absalon, J., Gurtman, A., Lockhart, S., Perez, J.L., Perez Marc,
816 G., Moreira, E.D., Zerbini, C., et al. (2020). Safety and Efficacy of the BNT162b2 mRNA Covid-19
817 Vaccine. N Engl J Med *383*, 2603-2615. 10.1056/NEJMoa2034577.
818 Roberts, A., Deming, D., Paddock, C.D., Cheng, A., Yount, B., Vogel, L., Herman, B.D., Sheahan, T.,
819 Heise, M., Genrich, G.L., et al. (2007). A mouse-adapted SARS-coronavirus causes disease and mortality
820 in BALB/c mice. PLoS Pathog *3*, e5. 10.1371/journal.ppat.0030005.
821 Routhu, N.K., Cheedarla, N., Bollimpelli, V.S., Gangadhara, S., Edara, V.V., Lai, L., Sahoo, A.,
822 Shiferaw, A., Styles, T.M., Floyd, K., et al. (2021). SARS-CoV-2 RBD trimer protein adjuvanted with

823 Alum-3M-052 protects from SARS-CoV-2 infection and immune pathology in the lung. Nat Commun *12*,
824 3587. 10.1038/s41467-021-23942-y.
825 Saunders, K.O., Lee, E., Parks, R., Martinez, D.R., Li, D., Chen, H., Edwards, R.J., Gobeil, S., Barr, M.,
826 Mansouri, K., et al. (2021). Neutralizing antibody vaccine for pandemic and pre-emergent coronaviruses.
827 Nature *594*, 553-559. 10.1038/s41586-021-03594-0.
828 Schmidt, F., Weisblum, Y., Rutkowska, M., Poston, D., DaSilva, J., Zhang, F., Bednarski, E., Cho, A.,
829 Schaefer-Babajew, D.J., Gaebler, C., et al. (2021). High genetic barrier to SARS-CoV-2 polyclonal
830 neutralizing antibody escape. Nature *600*, 512-516. 10.1038/s41586-021-04005-0.
831 Smirnov, D., Schmidt, J.J., Capecchi, J.T., and Wightman, P.D. (2011). Vaccine adjuvant activity of 3M-
832 052: an imidazoquinoline designed for local activity without systemic cytokine induction. Vaccine *29*,
833 5434-5442. 10.1016/j.vaccine.2011.05.061.
834 Voysey, M., Clemens, S.A.C., Madhi, S.A., Weckx, L.Y., Folegatti, P.M., Aley, P.K., Angus, B., Baillie,
835 V.L., Barnabas, S.L., Bhorat, Q.E., et al. (2021). Safety and efficacy of the ChAdOx1 nCoV-19 vaccine
836 (AZD1222) against SARS-CoV-2: an interim analysis of four randomised controlled trials in Brazil,
837 South Africa, and the UK. Lancet *397*, 99-111. 10.1016/S0140-6736(20)32661-1.
838 Wang, L., and Cheng, G. (2021). Sequence analysis of the emerging SARS-CoV-2 variant Omicron in
839 South Africa. J Med Virol. 10.1002/jmv.27516.
840 Wolfel, R., Corman, V.M., Guggemos, W., Seilmaier, M., Zange, S., Muller, M.A., Niemeyer, D., Jones,
841 T.C., Vollmar, P., Rothe, C., et al. (2020). Virological assessment of hospitalized patients with COVID-
842 2019. Nature *581*, 465-469. 10.1038/s41586-020-2196-x.
843 Wrapp, D., Wang, N., Corbett, K.S., Goldsmith, J.A., Hsieh, C.L., Abiona, O., Graham, B.S., and
844 McLellan, J.S. (2020). Cryo-EM structure of the 2019-nCoV spike in the prefusion conformation. Science
845 *367*, 1260-1263. 10.1126/science.abb2507.
846 Yang, J., Wang, W., Chen, Z., Lu, S., Yang, F., Bi, Z., Bao, L., Mo, F., Li, X., Huang, Y., et al. (2020). A
847 vaccine targeting the RBD of the S protein of SARS-CoV-2 induces protective immunity. Nature *586*,
848 572-577. 10.1038/s41586-020-2599-8.

849 Yu, J., Tostanoski, L.H., Peter, L., Mercado, N.B., McMahan, K., Mahrokhian, S.H., Nkolola, J.P., Liu,
850 J., Li, Z., Chandrashekar, A., et al. (2020). DNA vaccine protection against SARS-CoV-2 in rhesus
851 macaques. Science *369*, 806-811. 10.1126/science.abc6284.
852 Zhou, T., Teng, I.T., Olia, A.S., Cerutti, G., Gorman, J., Nazzari, A., Shi, W., Tsybovsky, Y., Wang, L.,
853 Wang, S., et al. (2020). Structure-Based Design with Tag-Based Purification and In-Process Biotinylation
854 Enable Streamlined Development of SARS-CoV-2 Spike Molecular Probes. Cell Rep *33*, 108322.
855 10.1016/j.celrep.2020.108322.
856 Zivanov, J., Nakane, T., Forsberg, B.O., Kimanius, D., Hagen, W.J., Lindahl, E., and Scheres, S.H.
857 (2018). New tools for automated high-resolution cryo-EM structure determination in RELION-3. Elife *7*.
858 10.7554/eLife.42166.
859

Figure 1

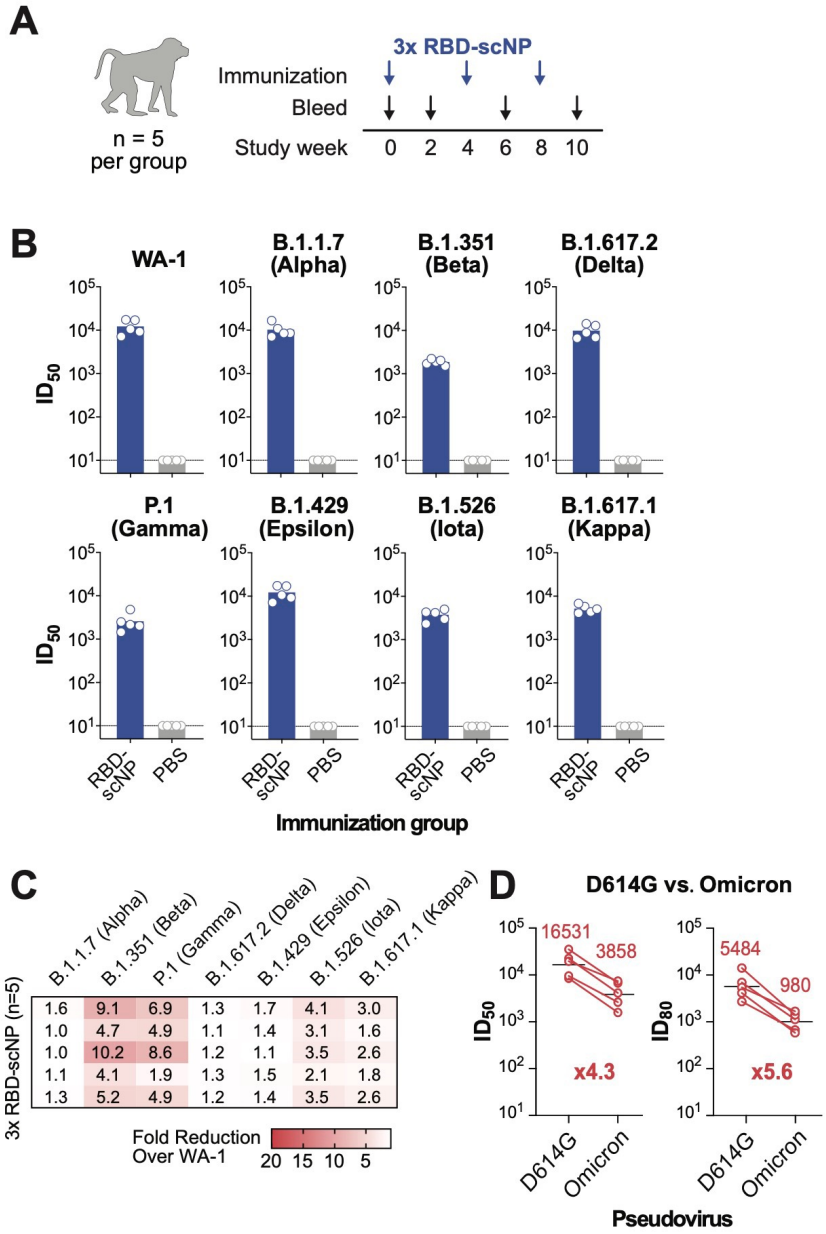

Figure 1. RBD-scNP vaccination elicits broad neutralizing antibodies against SARS-CoV-2 variants.

(A) Schematic of the vaccination study in macaques. Cynomolgus macaques (*n* = 5 per group) were immunized intramuscularly 3 times with 100 µg of RBD-scNP adjuvanted with 3M-052-AF + Alum. The control group was immunized with PBS. Blood and mucosal samples, including Bronchoalveolar lavage (BAL) and nasal swab samples, were collected in the indicated time points for antibody assays.

(B-C) Plasma antibody (post-3rd immunization) neutralization of SARS-CoV-2 variants pseudovirus infection of 293T-ACE2-TMPRSS2 cells. (B) Neutralization titers were shown as 50% inhibitory dilution (ID50). (C) Reduction of neutralization titers against variants were shown as fold reduction compared to the titers against WA-1.

(D) Plasma antibody (post-3rd immunization) neutralization titers against pseudoviruses of the SARS-CoV-2 Omicron variants in 293T-ACE2 cells. The mean ID50 and ID80 titers and the fold reduction compared to D614G are shown.

Figure 2

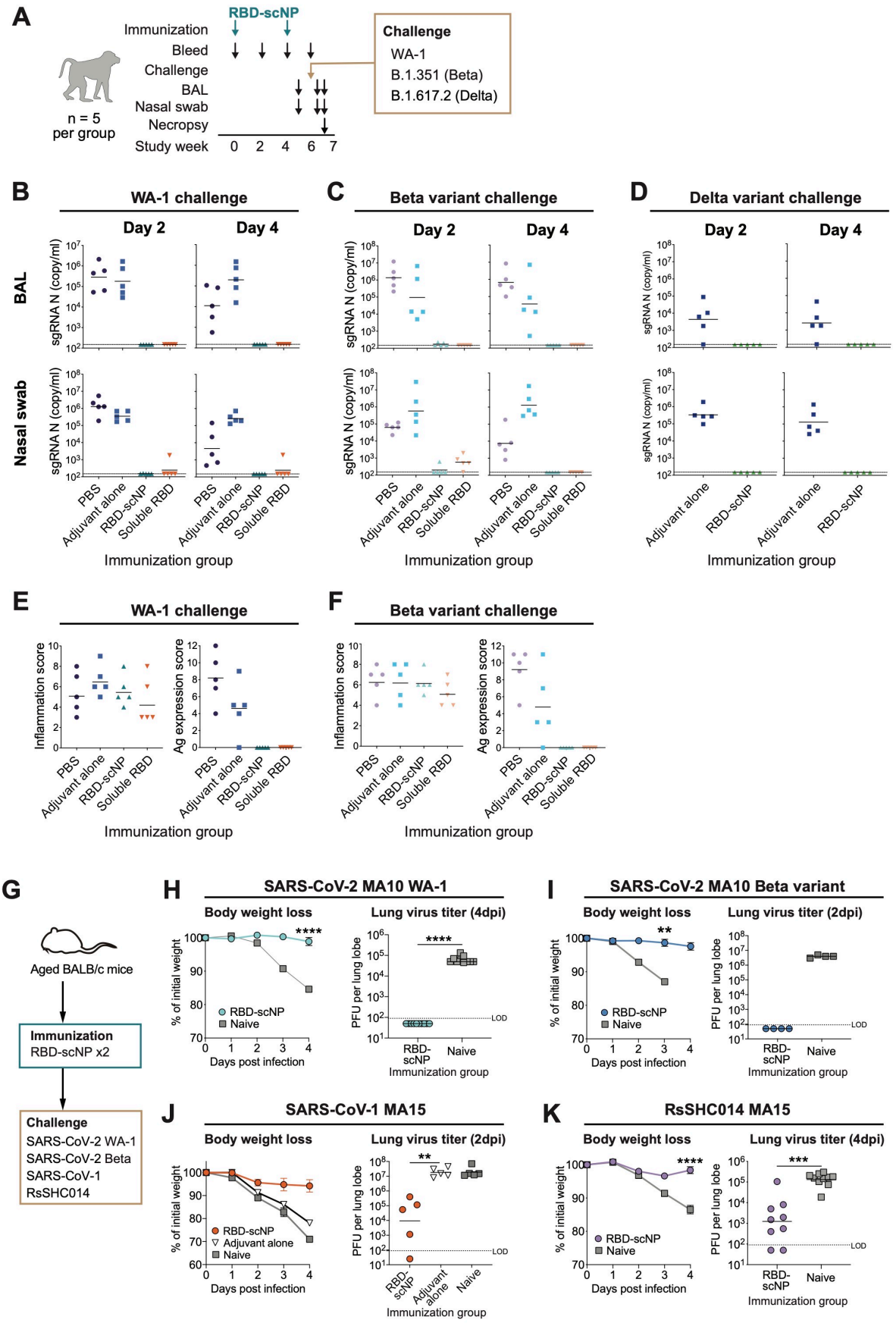
A
RBD-scNP
Immunization
Bleed
Challenge
BAL
Nasal swab
Necropsy
Study week
0 2 4 6 7
n = 5 per group
Challenge
WA-1
B.1.351 (Beta)
B.1.617.2 (Delta)
B
WA-1 challenge
Day 2
Day 4
BAL
Nasal swab
sgRNA N (copy/ml)
PBS
Adjuvant alone
RBD-scNP
Soluble RBD
Immunization group
C
Beta variant challenge
D
Delta variant challenge
E
WA-1 challenge
Inflammation score
Ag expression score
F
Beta variant challenge
G
Aged BALB/c mice
Immunization
RBD-scNP x2
Challenge
SARS-CoV-2 WA-1
SARS-CoV-2 Beta
SARS-CoV-1
RsSHC014
H
SARS-CoV-2 MA10 WA-1
Body weight loss
Lung virus titer (4dpi)
% of initial weight
Days post infection
RBD-scNP
Naive
PFU per lung lobe
LOD
I
SARS-CoV-2 MA10 Beta variant
Lung virus titer (2dpi)
J
SARS-CoV-1 MA15
Adjuvant alone
K
RsSHC014 MA15
Lung virus titer (4dpi)

Figure 2. Two doses of RBD-scNP vaccination protected non-human primates and mice from challenges of SARS-CoV-2 variants and other betacoronaviruses.

(A) Schematic of the non-human primate challenge studies. Cynomolgus macaques were immunized with 2 doses of RBD-scNP adjuvanted with 3M-052-AF + Alum or the indicated negative controls. Monkeys were intranasally and intratracheally challenged with SARS-CoV-2 WA-1 strain (n=5) or B.1.351 (n=5) or B.1.617.2 (n=5) at week 6. Lower and upper respiratory tract samples were collected on day 0, 2 and 4 post challenge for subgenomic (sgRNA) viral replication test. Animals were necropsied on day 4 post-challenge and organs were collected for pathologic analysis.

(B-D) SARS-CoV-2 subgenomic RNA (sgRNA) levels for nucleocapsid (N) gene in BAL (upper row) and nasal swab (lower row) samples collected on Day 2 and 4 after SARS-CoV-2 WA-1 virus challenge, SARS-CoV-2 WA-1 (B), Beta variant challenge (C) or Delta variant challenge (D). Dashed line indicates limit of the detection (150 copies/ml).

(E-F) Histopathological analysis of the SARS-CoV-2 WA-1 virus challenged (E) and the Beta variant challenged (F) animals. Lung sections from each animal were scored for inflammation by hematoxylin and eosin (H&E) staining, and for the presence of SARS-CoV-2 nucleocapsid by immunohistochemistry (IHC) staining.

(G) Schematic of the mouse challenge studies. Aged female BALB/c mice (n=10 per group) were immunized intramuscularly with adjuvanted RBD-scNP twice and challenged with SARS-CoV-2 mouse-adapted 10 (MA10) WA-1, SARS-CoV-2 MA10 Beta variant, SARS-CoV-1 mouse-adapted 15 (MA15), or Bat CoV RsSHC014 MA15. Body weights were monitored daily and lungs virus titer were measured in one lung lobe collected 2 days post-infection (dpi) or 4 dpi as indicated.

(H) Weight loss and lung virus titers at 4 dpi of the SARS-CoV-2 MA10 WA-1 challenged mice.

(I) Weight loss and lung virus titers at 2 dpi of the SARS-CoV-2 MA10 Beta variant challenged mice.

(J) Weight loss and lung virus titers at 2 dpi of the SARS-CoV-1 MA15 challenged mice.

(K) Weight loss and lung virus titers at 4 dpi of the Bat CoV RsSHC014 MA15 challenged mice.

ns, not significant, *P<0.05, **P<0.01, ***P<0.001, ****P<0.0001, Wilcoxon rank sum exact test. LOD: Limit of detection.

Figure 3

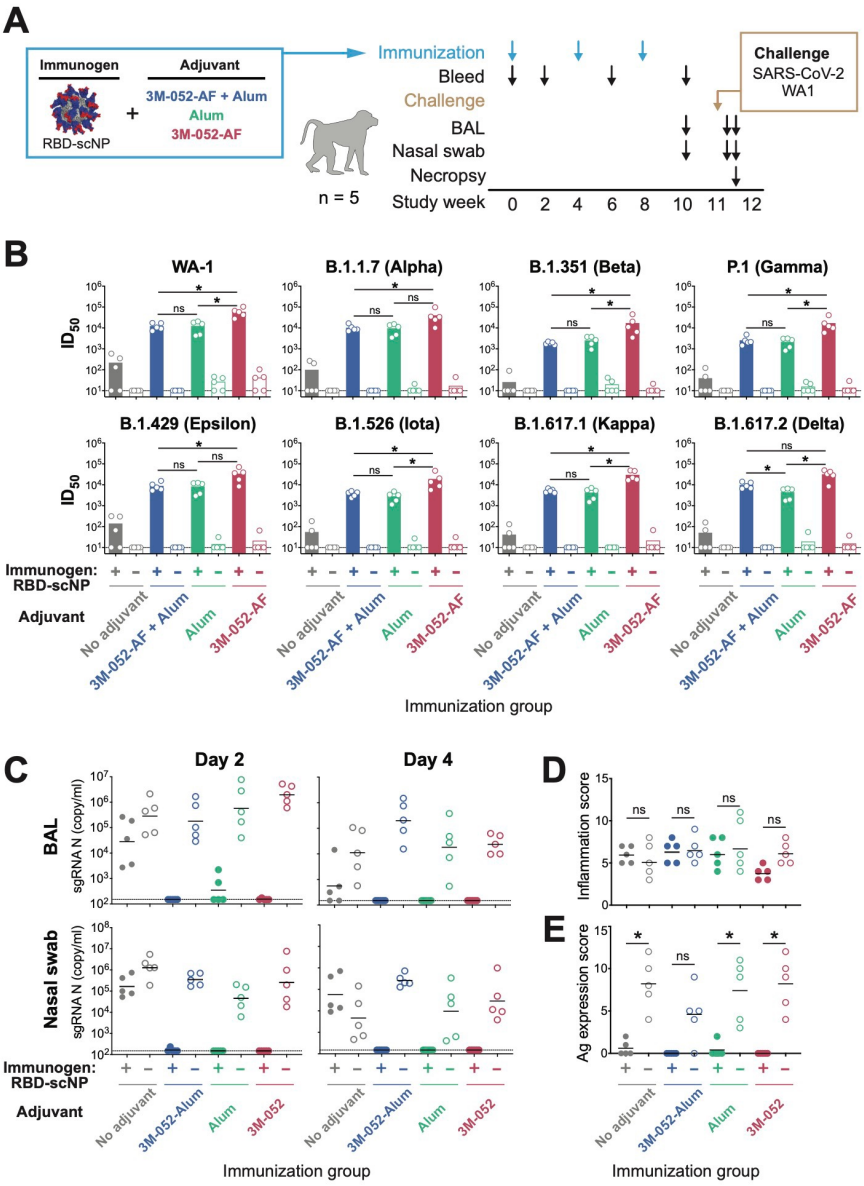

Figure 3. Neutralizing antibodies and *in vivo* protection elicited by RBD-scNP vaccine formulated with three different adjuvants.

(A) Schematic of the vaccination and viral challenge study. Cynomolgus macaques (n = 5 per group) were immunized intramuscularly for 3 doses with 100 µg of RBD-scNP adjuvanted with 3M052-AF + Alum, Alum, 3M052-AF, or PBS control. Animals injected with adjuvant alone or PBS were set as control groups. Monkeys were intranasally and intratracheally challenged with SARS-CoV-2 WA-1 at week 11. Blood samples were collected in week 0, 2, 6, 10. Lower and upper respiratory tract samples were collected on day 0, 2 and 4 post challenge for subgenomic RNA (sgRNA) viral replication test. Animals were necropsied on day 4 post-challenge, and organs were collected for pathologic analysis.

(B) Vaccine-induced neutralization titers against SARS-CoV-2 WA-1 and variants. Plasma samples collected after the third vaccination were tested in neutralization assays against pseudovirus viruses in 293T-ACE2-TMPRSS2. Neutralization titers were shown as 50% inhibitory dilution (ID50). ns, not significant, *P<0.05, Wilcoxon rank sum exact test.

(C) SARS-CoV-2 sgRNA viral replication assays. SARS-CoV-2 N gene sgRNA were quantified in BAL (upper row) and nasal swab (lower row) samples collected on day 2 and 4 post-challenge. Dashed line indicates limit of the detection (150 copies/ml).

(D-E) Histopathological analysis of the challenged animals. Lung sections from each animal were scored for lung inflammation by H&E staining (D), and for the presence of SARS-CoV-2 nucleocapsid by IHC staining (E). ns, not significant, *P<0.05, Wilcoxon rank sum exact test.

Figure 4

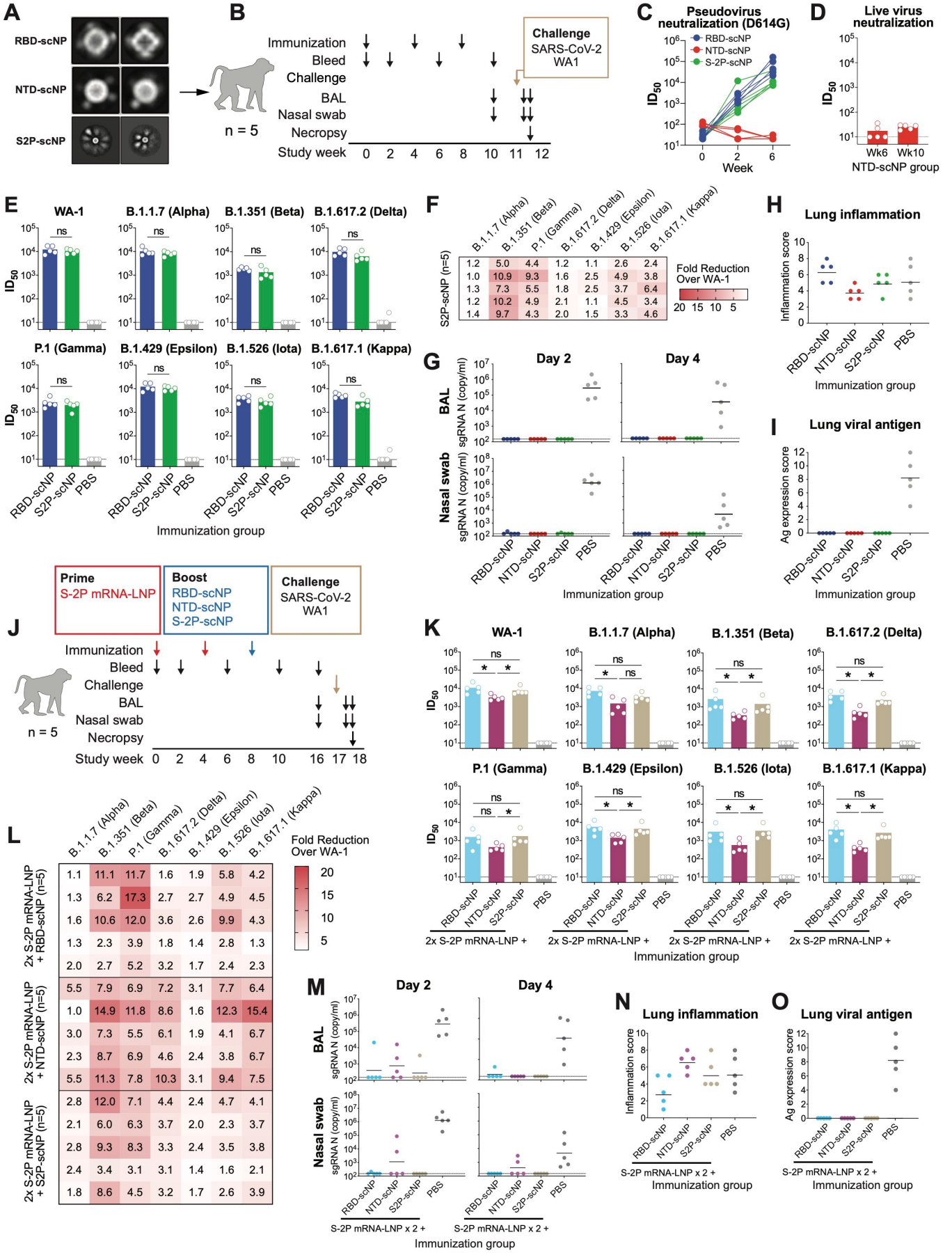
A
RBD-scNP
NTD-scNP
S2P-scNP
B
n = 5
Immunization
Bleed
Challenge
BAL
Nasal swab
Necropsy
Study week
0 2 4 6 8 10 11 12
Challenge
SARS-CoV-2
WA1
C
Pseudovirus neutralization (D614G)
RBD-scNP
NTD-scNP
S2P-scNP
ID50
Week
D
Live virus neutralization
ID50
Wk6
Wk10
NTD-scNP group
E
WA-1
B.1.1.7 (Alpha)
B.1.351 (Beta)
B.1.617.2 (Delta)
P.1 (Gamma)
B.1.429 (Epsilon)
B.1.526 (Iota)
B.1.617.1 (Kappa)
ns
ID50
RBD-scNP
S2P-scNP
PBS
Immunization group
F
B.1.1.7 (Alpha)
B.1.351 (Beta)
P.1 (Gamma)
B.1.617.2 (Delta)
B.1.429 (Epsilon)
B.1.526 (Iota)
B.1.617.1 (Kappa)
S2P-scNP (n=5)
1.2 5.0 4.4 1.2 1.1 2.6 2.4
1.0 10.9 9.3 1.6 2.5 4.9 3.8
1.3 7.3 5.5 1.8 2.5 3.7 6.4
1.2 10.2 4.9 2.1 1.1 4.5 3.4
1.4 9.7 4.3 2.0 1.5 3.3 4.6
Fold Reduction Over WA-1
20 15 10 5
G
Day 2
Day 4
BAL
Nasal swab
sgRNA N (copy/ml)
RBD-scNP
NTD-scNP
S2P-scNP
PBS
Immunization group
H
Lung inflammation
Inflammation score
RBD-scNP
NTD-scNP
S2P-scNP
PBS
Immunization group
I
Lung viral antigen
Ag expression score
RBD-scNP
NTD-scNP
S2P-scNP
PBS
Immunization group
J
Prime
S-2P mRNA-LNP
Boost
RBD-scNP
NTD-scNP
S-2P-scNP
Challenge
SARS-CoV-2
WA1
n = 5
Immunization
Bleed
Challenge
BAL
Nasal swab
Necropsy
Study week
0 2 4 6 8 10 16 17 18
K
WA-1
B.1.1.7 (Alpha)
B.1.351 (Beta)
B.1.617.2 (Delta)
P.1 (Gamma)
B.1.429 (Epsilon)
B.1.526 (Iota)
B.1.617.1 (Kappa)
ns
*
ID50
RBD-scNP
NTD-scNP
S2P-scNP
PBS
2x S-2P mRNA-LNP +
Immunization group
L
B.1.1.7 (Alpha)
B.1.351 (Beta)
P.1 (Gamma)
B.1.617.2 (Delta)
B.1.429 (Epsilon)
B.1.526 (Iota)
B.1.617.1 (Kappa)
2x S-2P mRNA-LNP + RBD-scNP (n=5)
1.1 11.1 11.7 1.6 1.9 5.8 4.2
1.3 6.2 17.3 2.7 2.7 4.9 4.5
1.6 10.6 12.0 3.6 2.6 9.9 4.3
1.3 2.3 3.9 1.8 1.4 2.8 1.3
2.0 2.7 5.2 3.2 1.7 2.4 2.3
2x S-2P mRNA-LNP + NTD-scNP (n=5)
5.5 7.9 6.9 7.2 3.1 7.7 6.4
1.0 14.9 11.8 8.6 1.6 12.3 15.4
3.0 7.3 5.5 6.1 1.9 4.1 6.7
2.3 8.7 6.9 4.6 2.4 3.8 6.7
5.5 11.3 7.8 10.3 3.1 9.4 7.5
2x S-2P mRNA-LNP + S2P-scNP (n=5)
2.8 12.0 7.1 4.4 2.4 4.7 4.1
2.1 6.0 6.3 3.7 2.0 2.3 3.7
2.8 9.3 8.3 3.3 2.4 3.5 3.8
2.4 3.4 3.1 3.1 1.4 1.6 2.1
1.8 8.6 4.5 3.2 1.7 2.6 3.9
Fold Reduction Over WA-1
20
15
10
5
M
Day 2
Day 4
BAL
Nasal swab
sgRNA N (copy/ml)
RBD-scNP
NTD-scNP
S2P-scNP
PBS
S-2P mRNA-LNP x 2 +
Immunization group
N
Lung inflammation
Inflammation score
RBD-scNP
NTD-scNP
S2P-scNP
PBS
S-2P mRNA-LNP x 2 +
Immunization group
O
Lung viral antigen
Ag expression score
RBD-scNP
NTD-scNP
S2P-scNP
PBS
S-2P mRNA-LNP x 2 +
Immunization group

Figure 4. Neutralizing antibodies and *in vivo* protection induced by RBD-scNP, NTD-scNP and S2P-scNP vaccines as a three-dose regimen or as a heterologous boost for S2P mRNA-LNP vaccine.

(A) Negative-stain electron microscopy of RBD-scNP, NTD-scNP, and S2P-scNP. The insets show zoomed-in image of a representative scNPs. The 2D class averaging of 14,300 RBD-scNP particles, 10,800 NTD-scNP particles or 1,034 S2P-scNP particles were generated using RELION. The size of each box is 257 Å, 257 Å, and 1,029 Å for RBD-scNP, NTD-scNP and S2P-scNP, respectively.

(B) Schematic of the RBD-scNP, NTD-scNP and S2P-scNP immunization study. Cynomolgus macaques (n = 5 per group) were immunized intramuscularly for 3 times with 100 µg of RBD-scNP, NTD-scNP, or S2P-scNP adjuvanted with 3M-052-AF + Alum. The control group was immunized with PBS. Blood samples were collected at weeks 0, 2, 6, 10 and monkeys were intranasally and intratracheally challenged with SARS-CoV-2 WA-1 strain at week 11. Lower and upper respiratory tract samples were collected on days 0, 2 and 4 post-challenge for sub-genomic (sgRNA) RNA viral replication assays. Animals were necropsied on day 4 post-challenge, and organs were collected for pathologic analysis.

(C) Pseudovirus neutralization. Plasma samples collected in week 0, 2, 6 were tested in neutralization assays against pseudotyped SARS-CoV-2 D614G strain in 293T/ACE2.MF cells.

(D) Live virus neutralization of the NTD-scNP-induced antibodies. Plasma samples from the NTD-scNP group collected in week 6 and 10 were tested in neutralization assays against live SARS-CoV-2 virus in Vero-E6 cells.

(E-F) Plasma antibody neutralization titers against pseudoviruses of the SARS-CoV-2 variants in 293T-ACE2-TMPRSS2 cells. (E) Neutralization titers were shown as 50% inhibitory dilution (ID50). ns, not significant, *P<0.05, Wilcoxon rank sum exact test. (F) Reduction of neutralization titers of the S2P-scNP group against variants were shown as fold changes over the titers against WA-1. Statistical significance in all the panels were determined using Wilcoxon rank sum exact test. Asterisks show the statistical significance: ns, not significant.

(G) SARS-CoV-2 sgRNA levels for the N gene in BAL (upper row) and nasal swab (lower row) samples collected on Day 2 and 4 post-challenge.

(H-I) Histopathological analysis of the challenged animals. Lung sections from each animal were scored for inflammation by H&E staining (H), and for the presence of SARS-CoV-2 nucleocapsid by IHC staining (I).

(J) Schematic of the heterologous prime-boost vaccination study. Cynomolgus macaques (n = 5 per group) were immunized intramuscularly with 2 doses of S-2P mRNA-LNP vaccine, then boosted with 100 µg of RBD-scNP, NTD-scNP, or S2P-scNP adjuvanted with 3M-052-AF + Alum. Animals in the control group were immunized with PBS. Blood samples were collected in week 0, 2, 6, 10, 16, and monkeys were intranasally and intratracheally challenged with SARS-CoV-2 WA-1 strain at week 17. Lower and upper respiratory tract samples were collected on day 0, 2 and 4 post challenge for sgRNA viral replication test. Animals were necropsied on day 4 post-challenge for pathologic analysis.

(K-L) Plasma antibody neutralization titers against pseudoviruses of the SARS-CoV-2 variants in 293T-ACE2-TMPRSS2 cells. (K) Neutralization titers were shown as 50% inhibitory dilution (ID_{50}). ns, not significant, *P<0.05, Wilcoxon rank sum exact test. (L) Reduction of neutralization titers against variants were shown as fold changes over the titers against WA-1. Animal groups and animal IDs were indicated on the left. Statistical significance in all the panels were determined using Wilcoxon rank sum exact test. Asterisks show the statistical significance: ns, not significant, *P<0.05.

(M) SARS-CoV-2 sgRNA levels for N gene in BAL (upper row) and nasal swab (lower row) samples collected before challenge and on Day 2 and 4 post-challenge.

(N-O) Histopathological analysis of the challenged animals. Lung sections from each animal were scored for inflammation by H&E staining (N), and for the presence of SARS-CoV-2 nucleocapsid by IHC staining (O).

Supplementary Figure 1

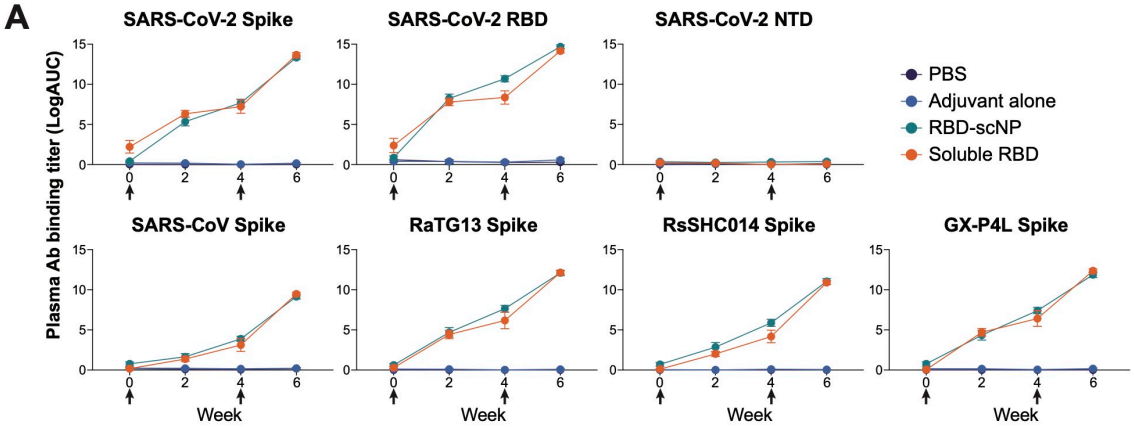

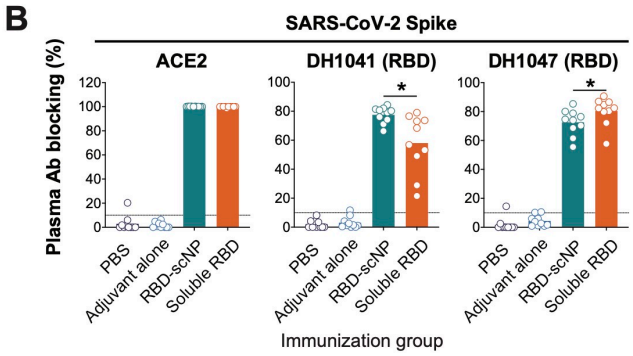

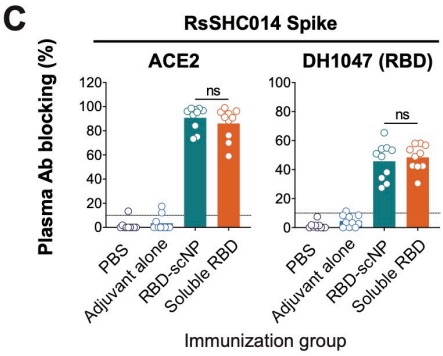

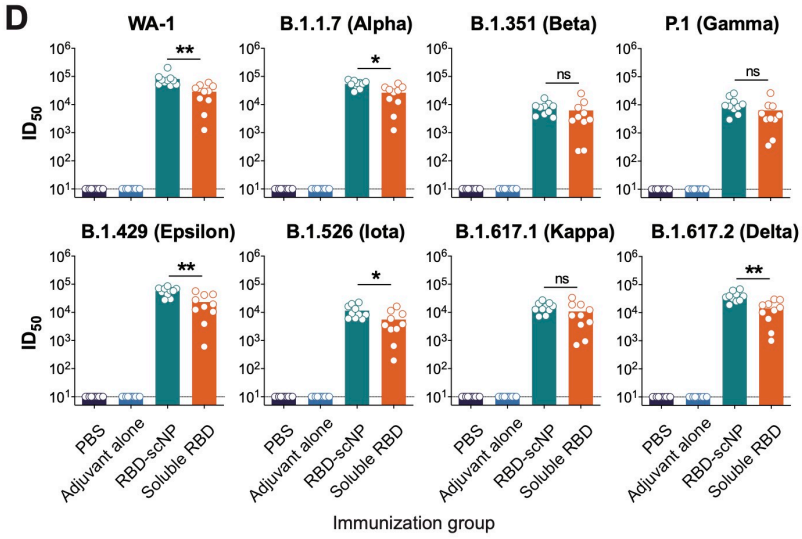

E

	B.1.1.7 (Alpha)	B.1.351 (Beta)	P.1 (Gamma)	B.1.617.2 (Delta)	B.1.429 (Epsilon)	B.1.526 (Iota)	B.1.617.1 (Kappa)
2x RBD-scNP (n=10)	1.6	5.7	12.2	2.5	1.1	10.6	3.7
	1.0	9.1	14.9	1.3	1.5	17.2	6.8
	1.2	3.2	4.8	1.6	0.9	4.0	3.2
	2.9	10.3	24.1	4.5	2.7	9.9	15.8
	2.3	7.3	13.8	2.5	1.1	8.8	8.8
	1.0	11.7	13.0	2.6	1.0	8.5	6.0
	1.1	8.0	8.3	2.1	1.3	7.0	4.4
	1.4	14.4	11.0	1.2	3.1	9.7	4.2
	1.3	3.4	4.5	1.9	1.2	3.0	3.5
	1.1	7.2	10.7	1.6	1.8	10.3	3.5
2x soluble RBD (n=10)	1.1	5.0	6.4	3.0	1.1	5.3	3.2
	1.1	3.8	6.1	2.5	1.5	5.0	3.9
	0.9	7.9	9.6	2.8	2.8	11.7	6.4
	1.1	5.8	4.7	2.4	1.1	4.1	3.9
	1.1	18.9	7.8	2.3	1.1	6.6	6.1
	1.1	9.1	5.0	1.5	1.1	5.1	3.7
	1.0	5.4	3.5	1.3	2.1	6.4	1.3
	1.2	2.0	1.9	2.7	1.1	3.0	1.5
	1.0	5.6	5.1	1.1	1.0	6.4	2.1
	1.1	14.0	8.8	1.3	1.4	9.9	2.0

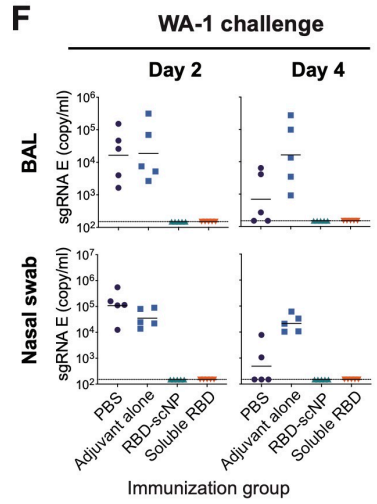

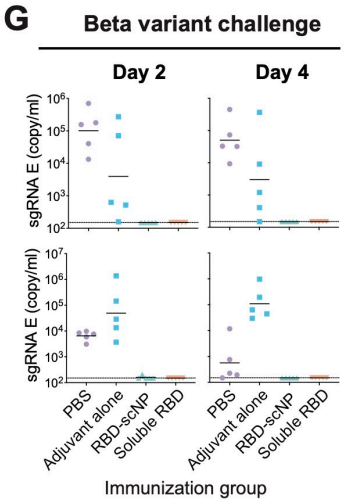

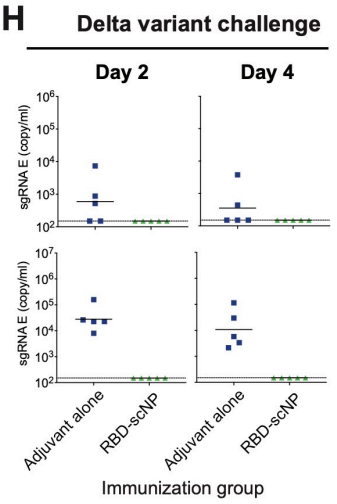

Supplementary Figure 1. RBD-scNP elicited higher titers of neutralizing antibodies than soluble RBD. Related to Figure 2.

(A) Plasma antibody binding titers to SARS-CoV-2 spike, RBD and NTD, as well as spike proteins of SARS-CoV, bat coronaviruses RaTG13, RsSHC014, and pangolin coronavirus GX-P4L. ELISA binding titers were shown by log area-under-curve (AUC). Dot and error bars indicate mean ± SEM of all animals in each group.

(B-C) Plasma antibody blocking activity after the 2nd immunization. ELISA was performed to test plasma antibodies blocking ACE2, human RBD neutralizing antibodies DH1041 and DH1047 binding to SARS-CoV-2 Spike protein (B), or plasma samples blocking ACE2, DH1041 and DH1047 binding to RsSHC014 Spike protein (C). Data are expressed as percentages of blocking of ACE or the indicated antibody by 1:50 diluted plasma samples.

(D-E) Plasma antibody neutralization titers against pseudoviruses of the SARS-CoV-2 variants in 293T-ACE2-TMPRSS2 cells. (D) Neutralization titers were shown as 50% inhibitory dilution (ID_{50}). (E) Reduction of neutralization titers against variants were shown as fold changes over the titers against WA-1.

(F-H) SARS-CoV-2 E sgRNA in BAL and nasal swab samples from the WA-1 (F), Beta variant (G), and Delta variant (H) challenged monkeys. Dashed line indicates limit of the detection (150 copies/ml).

ns, not significant, *P<0.05, Wilcoxon rank sum exact test.

Supplementary Figure 2

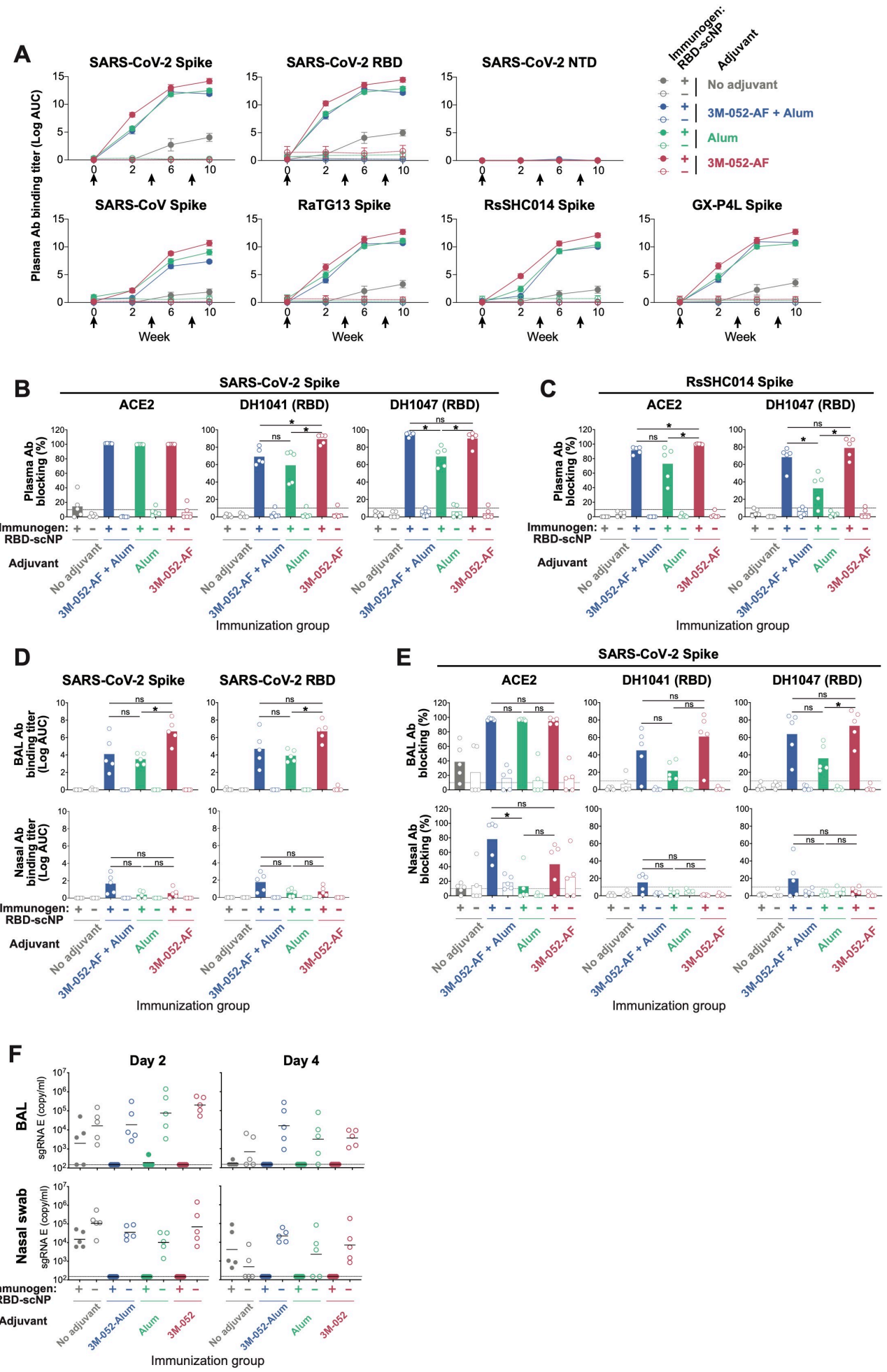

Supplementary Figure 2. Serum and mucosal antibody responses elicited by RBD-scNP formulated with three different adjuvants. Related to Figure 3.

(A) Plasma antibody binding titers. ELISA was performed to test plasma samples binding to SARS-CoV-2 spike, RBD and NTD, as well as spike proteins of SARS-CoV, bat coronaviruses RaTG13, RsSHC014, and pangolin coronavirus GX-P4L. ELISA binding titers were shown by mean ± SEM of log area-under-curve (AUC).

(B-C) Plasma antibody blocking activities after the 3rd immunization. ELISA was performed to test plasma samples blocking ACE2, human RBD neutralizing antibodies DH1041 and DH1047 binding to SARS-CoV-2 spike protein (B), or plasma samples blocking ACE2 and DH1047 binding to RsSHC014 spike protein (C). Data are expressed as percentages of blocking of ACE or the indicated antibody by 1:50 diluted plasma samples.

(D) Mucosal antibody binding titers in the lower and upper respiratory tracts after the 3rd immunization. ELISA was performed to test 10x concentrated bronchoalveolar lavage (BAL) or unconcentrated nasal wash samples binding to SARS-CoV-2 spike and RBD. ELISA binding titers are expressed as log AUC.

(E) Mucosal antibody blocking activities in the lower respiratory tracts after the 3rd immunization. ELISA for 10x concentrated BAL or unconcentrated nasal wash samples blocking ACE2, DH1041 and DH1047 binding to SARS-CoV-2 spike protein were performed, and percentages of blocking of ACE or the indicated antibody were shown.

(F) SARS-CoV-2 E sgRNA in BAL and nasal swab samples from WA-1 challenged monkeys. Dashed line indicates limit of the detection (150 copies/ml).

ns, not significant, *$P<0.05$, Wilcoxon rank sum exact test.

Supplementary Figure 3

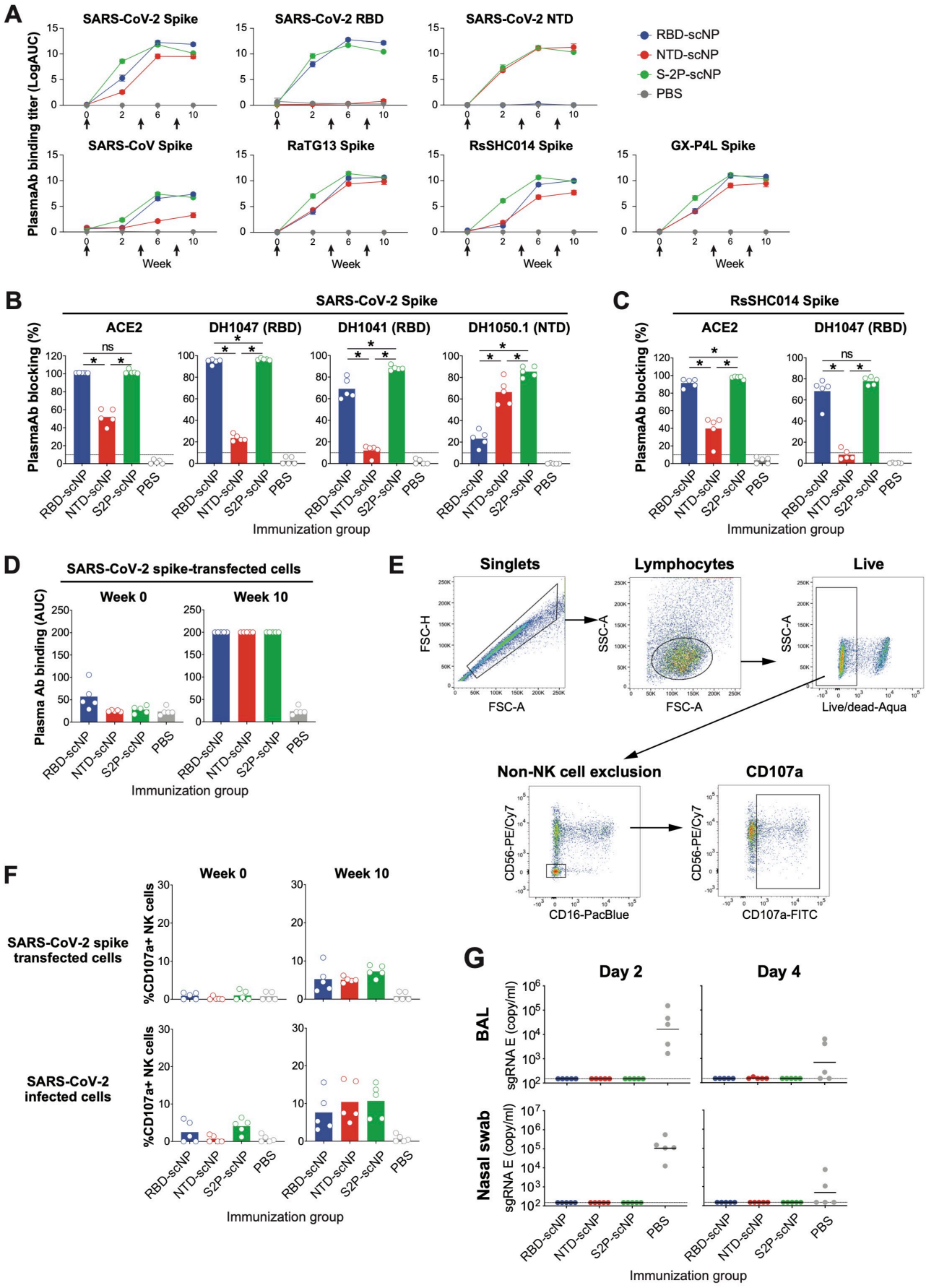

Supplementary Figure 3. RBD-scNP, NTD-scNP and S2P-scNP induced spike-specific binding antibodies and mediated ADCC. Related to Figure 4.

(A) Plasma antibody binding titers. ELISA was performed to test plasma samples binding to SARS-CoV-2 spike, RBD or NTD recombinant proteins, as well as to spike proteins of SARS-CoV, bat coronaviruses RaTG13, RsSHC014, and pangolin coronavirus GX-P4L. ELISA binding titers were are expressed as log area-under-curve (AUC). Dot and error bars indicate mean ± SEM of all animals in each group.

(B-C) Plasma antibody blocking activity after the 3rd immunization. ELISA was performed to test plasma antibodies blocking ACE2, human RBD neutralizing antibodies DH1041 and DH1047, and human NTD neutralizing antibody DH1050.1 binding to SARS-CoV-2 spike protein (B), or plasma samples blocking ACE2, DH1041 and DH1047 binding to RsSHC014 spike protein (C). Data are expressed as percentages of blocking of ACE or the indicated antibody by 1:50 diluted plasma samples. ns, not significant, *P<0.05, Wilcoxon rank sum exact test.

(D) Plasma antibodies staining on SARS-CoV-2 spike-transfected 293T cells. Pre-immunization (week 0) and pre-challenge (week 10) samples were tested.

(E) The gating strategy for the NK cell degranulation ADCC assay. Purified human NK cells were mixed with SARS-CoV-2 spike-transfected cells or SARS-CoV-2 infected cells in the presence of 1:500 diluted plasma samples. NK cell degranulation was detected based on CD107a expression.

(F) RBD-scNP-, NTD-scNP- and S2P-scNP-induced antibodies mediated ADCC. The percentages of CD107a+ NK cells were shown when NK cells were assayed with plasma antibodies in SARS-CoV-2 spike transfected 293T cells (top row) or SARS-CoV-2 infected Vero E6 cells cells (botton row).

(G) SARS-CoV-2 E sgRNA in BAL and nasal swab samples from WA-1 challenged monkeys. Dashed line indicates limit of the detection (150 copies/ml).

Supplementary Figure 4

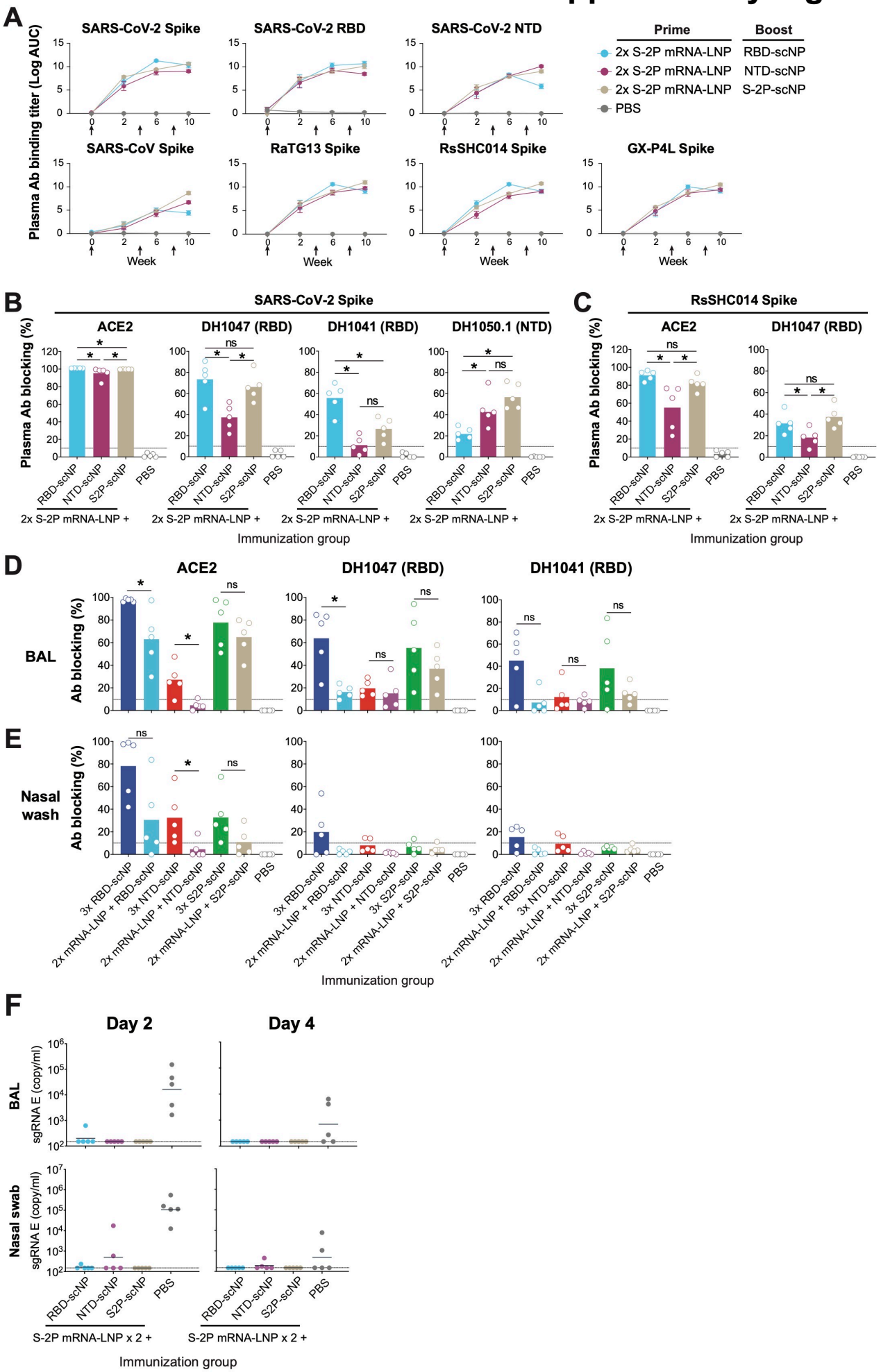

Supplementary Figure 4. Antibody responses elicited by scNP vaccines as a booster vaccination in macaques that received two doses of S-2P mRNA-LNP vaccine. Related to Figure 4.

(A) Plasma antibody binding titers. ELISA was performed to test plasma antibodies binding to SARS-CoV-2 spike, RBD and NTD, as well as spike proteins of SARS-CoV, bat coronaviruses RaTG13, RsSHC014, and pangolin coronavirus GX-P4L. ELISA binding titers were shown by log area-under-curve (AUC). Dot and error bars indicate mean ± SEM of all animals in each group.

(B-C) Plasma antibody blocking activity after the 3rd immunization. ELISA was performed to test plasma antibodies blocking ACE2, human RBD neutralizing antibodies DH1041 and DH1047, and human NTD antibody DH1050.1 binding to SARS-CoV-2 spike protein (B), or plasma samples blocking ACE2, DH1041 and DH1047 binding to RsSHC014 spike protein (C). Data are expressed as percentages of blocking of ACE or the indicated antibody by 1:50 diluted plasma samples.

(D-E) Comparison of mucosal antibody blocking activities induced by 3 doses of scNP vaccination or 2 doses of S2P mRNA-LNP + 1 dose of scNP vaccination. ELISA for 10x concentrated bronchoalveolar lavage (BAL) samples (D) and neat nasal wash samples (E) blocking the binding of ACE2 or neutralizing antibody (DH1041 or DH1047) on SARS-CoV-2 spike were performed. Data are expressed as percentages of blocking of ACE or the indicated antibody by mucosal samples.

(F) SARS-CoV-2 E sgRNA in BAL and nasal swab samples from WA-1 challenged monkeys. Dashed line indicates limit of the detection (150 copies/ml).

ns, not significant, *P<0.05, Wilcoxon rank sum exact test.